# Satellite or ground-based measurements for production of site specific hourly irradiance data: which is most accurate and where?

Diane Palmer *, Elena Koubli, Ian Cole, Tom Betts and Ralph Gottschalg
Centre for Renewable Energy Systems Technology, Loughborough University, LE11 3TU, UK
* Corresponding Author D.Palmer@lboro.ac.uk Tel. +44 (0)1509 635604
E.Koumpli@lboro.ac.uk, I.R.Cole@lboro.ac.uk, T.R.Betts@lboro.ac.uk, R.Gottschalg@lboro.ac.uk

## Abstract

Site-specific satellite-derived hourly global horizontal irradiance is compared with that obtained from extrapolation and interpolation of values measured by ground-based weather stations. A national assessment of three satellite models and two ground-based techniques is described. A number of physiographic factors are examined to allow identification of the optimal resource. The chief influences are determined as: factors associated with latitude; terrain ruggedness; and weather station clustering/density. Whilst these factors act in combination, weather station density was found to be fundamental for a country like the UK, with its ever-changing weather. The decision between satellite and ground-based irradiance data based on accuracy is not straightforward. It depends on the exactitude of the selected satellite model and the concentration of pyranometric stations.

**Keywords**: global horizontal irradiance, national assessment of irradiance models, weather station density, kriging, satellite-derived irradiance, solar radiation.

## 1. Introduction

Solar radiation data has many applications, such as solar energy system performance and bankability assessment, building design of passive heating, cooling and daylighting elements, and resource assessment for agriculture and forestry. The most reliable i.e. lowest uncertainty source of solar radiation data is ground-based measurements by weather station networks and dedicated pyranometric stations (Sengupta et al., 2015). They measure the solar irradiance actually received at ground level, where solar systems are located. However, their reliability/uncertainty is conditional upon maintenance and calibration of the instruments. Pyranometer uncertainty must also be considered in the use of data.

This research investigates three methods to obtain solar radiation estimates for locations where it is not directly measured. The first is simply to allocate values from the single nearest measurement point. Here this method is termed “nearest neighbour extrapolation” (NNE) as in (Perez et al., 1997). Alternative names are “nearest neighbour interpolation”, “proximal interpolation” and “nearby station method”. The second method is to use an interpolation method based on the spatially weighted average of several neighbouring measurement locations. The third alternative approach is to model solar irradiance from cloud images captured by satellite. Like ground-based measurements, satellite data also has disadvantages. One shortcoming is lower accuracy at the specific weather location because the satellite data represents an area of the given pixel size, rather than an exact point.

There are no overall guidelines to direct the choice between ground-based or satellite irradiance data (Meteonorm, n.d.). This research sets out a data-informed methodology to aid the decision-making process and applies it to the UK as an example. It provides an extensive nationwide validation of these two solar irradiance data sources on an hourly basis. The case study area is the entire UK. This is a non-homogeneous region in terms of climate and topography and irradiance values vary significantly across the country.

Previous work has focused on distance from weather station as a deciding factor in the preferred choice of data source. As the distance between the point of measurement and location where data is required increases, the likelihood of divergence of weather conditions at the two sites also increases. In general, a distance decay effect may be observed, due to weather fronts and terrain. A theoretical distance is reached at which the decreasing accuracy of the ground-based data equals and then falls below the otherwise less accurate satellite-modelled data. This cross-over or break-even distance was determined as 34 km for hourly averaged global horizontal irradiance (GHI) data in 1997 (Perez et al., 1997). This research is discussed in Appendix A.

This original work (Perez et al., 1997) referred to *nearest neighbour extrapolation* of ground data, whereas a number of well-known ground data sources (Meteonorm (Meteonorm, n.d.), PVGIS-classic (JRC, 2012)) use *geostatistical interpolation*. Interpolation techniques have been in existence for some time, but more powerful computers have enabled their widespread use and enhanced understanding. The last 20 years have seen considerable advances in satellite modelling also. Advances in networking and communication technology have led to increased availability of data of all types. In this context, this paper examines whether the historic break-even distance is still the best criterion on which to base a data source decision.

Other factors in the ground-based or satellite GHI data selection are: proximity to mountains and oceans; urbanisation (associated with high and changeable concentrations of aerosols and water vapour); high latitude; cloud cover (Hall and Hall, 2010; Perez et al., 2013; Suri and Cebecauer, 2014); and weather station density (Paulescu et al., 2013). The differences in accuracy of data derived from extrapolation/interpolation of ground-based sources and satellite-modelled data in these distinct regions have never (to the authors' knowledge) been quantified.

Both ground-based and satellite models are affected by orographic forcing when changes in elevation occur. When air is blown over mountains or hills, it is forced to rise. As it rises, it cools, becoming saturated with condensing water and forming a cloud, a phenomenon that is highly localised. Satellite models produce higher errors in coastal locations and are adversely affected by scattered cloud, especially at high latitudes (Perez et al., 2013). Broken cloud may mask the sun. Conversely, thin cloud close to the sun may enhance solar irradiance due to forward scattering (Yordanov et al, 2013).  Current satellite instruments cannot distinguish small broken clouds from large thin cloud (Cebecauer et al., 2010).

Satellite values may also fail to distinguish clouds in the presence of bright surfaces e.g. snow or ice cover, and some types of vegetation. Interpolation of ground data is subject to edge effects. In the case of the UK, the coast is also the edge boundary of the weather station network and correlation might be expected. The temporal granularity of hourly weather station data is too coarse to reflect cloud movements. Thus, it is not at all clear which GHI data source provides the best accuracy in which geographic circumstance. This research will investigate this issue.

The accuracy of both ground-based and satellite-modelled GHI will be assessed in terms of root mean square error (RMSE) and mean bias error (MBE). The following comparisons will be made: (1) pair-wise comparison of weather station reading to nearest weather station value; (2) interpolated ground-measurement to nearest weather station record at various distances; and (3) interpolated ground versus satellite-derived values under differing geographic scenarios.

In the following, an assessment of solar irradiance models is carried out to direct the decision between the use of extrapolated/interpolated ground-measured or satellite-modelled irradiance data. First, the impact of distance to weather station is investigated, followed by the influence of other atmospheric and topographical factors as detailed above.

This paper is structured as follows. Section 2 describes the data employed and quality control procedures performed upon it. Calculation of distance decay errors is detailed. Section 3.1 replicates former research with modern data. An investigation of the influence of distance on whether ground or satellite irradiance data is most accurate, is described. The previous research is then expanded upon and the results clearly visualised. Section 3.2 investigates the influence of atmospheric and topographic factors on whether ground or satellite irradiance data delivers the greater accuracy. These include locational and weather-related features. Finally, Section 4 summarises findings, interprets the results and offers conclusions.

# 2. Data and Methods

All data used is hourly global horizontal solar irradiance data for the complete year of 2014, unless otherwise stated. The case study area is the United Kingdom.

## *2.1 Ground Data Description*

Ground-based solar irradiance measurements available as hourly averages are used from the UK Meteorological Office Integrated Data Archive System - MIDAS (UK Met Office, 2006). The UK Met Office currently has a network of over 80 automatic weather stations throughout the UK which observe irradiance as well as other meteorological conditions. Figure 1 and Figure 2 provide details of UK weather stations distribution. It may be seen that the distribution is somewhat uneven. 30% of the stations are clustered in the South East and Midlands i.e. approximately one-third of the weather stations are positioned in one-fifth of the nation. In other words, although stations are typically about 40 km apart, this can more than double, particularly in Wales and Scotland. The weather stations distance distribution has a small positive skew, with slightly more inter-station distances of less than 20 km and slightly fewer greater than 80 km.

The instruments at these stations are CM11/CMP11 (Kipp&Zonen) pyranometers, calibrated by reference to absolute cavity radiometers, traceable to the world radiation standard. Weather station sensors predominantly rely on rainfall for cleaning.

Figure 1: Map of Weather Stations Distribution

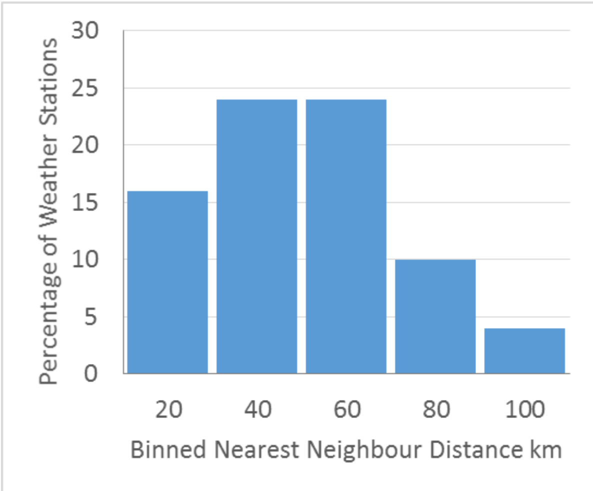


Figure 2: Histogram of Weather Stations Nearest Neighbour Distances

## *2.2 Ground Data Methodology*

The UK Met Office apply quality control procedures to MIDAS data before release. Data inputs automatically undergo checks to ensure that they are correct and consistent with the surrounding data points on entry to the Meteorological Monitoring System. Observations are compared to location-dependant climatological extremes and previous records. The downloaded MIDAS data was then filtered to remove duplicates, flagged error values and values less than 0 W/m$^2$. In addition, the following tests recommended by (Journée and Bertrand, 2011) where applied:

- The global horizontal solar radiation must be less than the extra-terrestrial value when the solar elevation angle is greater than 2 degrees.
- The global horizontal solar radiation must not exceed the European Solar Radiation Atlas clear sky value by more than 10% when the solar elevation angle is greater than 2 degrees.

It was determined that only 7 per 400,000 values were too high. This very small number of values was ignored.

The distance decay errors for nearest neighbour extrapolation and interpolation of data were calculated as follows. Firstly, the steps for NNE were: Take GHI values from two nearest neighbouring weather stations (1 and 2). Consider the value of station 2 to be unknown.

Accordingly, it becomes necessary to use the data from station 1. Validate the accuracy of station 1 data in these circumstances by comparing it to the real data from station 2. The distance decay is the distance between the two stations. This procedure is repeated for each closest weather station pair until all the data has been used. The RMSEs are plotted as a function of distance to nearest weather station. The NNE method is included in this research because this is the only method available to many GHI data users.

Secondly, interpolation distance decay errors were obtained. Interpolation takes the values from several weather stations surrounding the point of interest. These are input into a mathematical algorithm and weighted according to distance to the desired location to calculate a GHI value for the unknown site. This paper employs the kriging interpolation technique, detailed in Appendix B. The reduction in accuracy of interpolation due to distance decay is assessed by leave-one-out-cross-validation (LOOCV). This may be applied as follows: Interpolate with 79 weather stations and leave the 80$^{th}$ out. Compare the interpolated value obtained at the 80$^{th}$ station with the measured value from that site. (Calculate the RMSE). This is repeated for all stations (i.e. 80 times). Plot the RMSEs as a function of distance.

In this instance it is not sufficient to simply use the closest station distance to study loss of similarity between interpolated values with increasing distance. This is because GHI values from all weather stations are used in the kriging algorithm, not just those from closest to the location. Therefore, distance is obtained by re-using the kriging algorithm. The weather stations are treated individually. For each weather station, the distances to the other 79 weather stations are calculated. These values are then interpolated to obtain a value for the weather station of interest. This is repeated for all stations. The average difference between the closest station distance and interpolated distance was 11 km, and the maximum 56 km, for the 79 weather stations.

### *2.3 Satellite Irradiance Source*

Models which generate irradiance from satellite observations may be classified as physical (Miller et al., 2013) or hybrid (Perez et al., 2013). Hybrid models are also generally referred to as semi-empirical. Physical models utilise radiative transfer equations and require detailed information on the composition of the earth's atmosphere (e.g. cloud vertical distribution and optical properties, gridded aerosol properties and water vapour) as inputs. Obtaining data of sufficient quality for accurate results can be problematic. Hybrid models combine regression between satellite reflectance and corresponding ground measurements with a simplified radiative transfer algorithm.

Three models are investigated here. (1) CAMS (Schroedter-Homscheidt, 2016) utilises the Heliosat-4 physical model for satellite image-to-ground irradiance conversion. CAMS irradiance data is available at 15 minute, hourly, daily and monthly intervals. Hourly data only is analysed here, in order to be comparable with the ground-based MIDAS data. CAMS has a spatial resolution of 0.05° (5.6 km) and, in addition to satellite images, requires the following atmospheric data as inputs: aerosol properties, total column water vapour and ozone. These are obtained in the form of 3-hourly satellite-derived values and re-analysed via look-up tables to produce higher temporal resolution data, together with the shorter timeframe cloud satellite images. (2) SARAH-E (Amillo et al., 2014) is a hybrid model, The data is available in hourly format. It has a spatial resolution of 0.05° and atmospheric input requirements similar to CAMS but uses long-term monthly modelled averages for the atmospheric data look-up tables. SARAH-E data was available for 11 years (2005-2015). (3) Solargis (Cebecauer et al., 2010; Šúri and Cebecauer, 2012) also uses a hybrid approach. Solargis irradiance data is available at 15 minute, 30 minute, hourly, daily and monthly intervals. Again, hourly data only is analysed in this research. In addition to daily modelled values of atmospheric optical depth, water vapour and ozone (which are re-analysed to shorter time intervals), it includes snow index, snow depth, elevation and terrain shading in the model. Satellite elevation data is available at higher grid resolution, enabling Solargis to deliver a spatial resolution of 250 m.

# 3. Results and Discussion

## *3.1 Influence of distance to weather station on ground or satellite irradiance data choice*

### *3.1.1 Replication of earlier work*

Initially, the example of (Perez et al., 1997) was replicated with modern data by plotting the nRMSE (normalised by mean of inputs) as a function of distance to produce a semi-variogram-like graph, illustrated in Figure 3. This same graph displays: (i) the nearest neighbour extrapolation nRMSE as a function of closest station distance; (ii) the kriging LOOCV nRMSE as a function of interpolated distance; and (iii) the satellite error level band for each of the three satellite models tested (CAMS, SARAH and Solargis). These satellite error ranges were taken from validation figures reported in the literature. Each model is compared to two UK BSRN stations, Lerwick and Camborne. Instruments at BSRN stations provide data of the highest available accuracy. Since these are at the UK's northern and southern extremities, nRMSE is considered to range between these values for the country as a whole.

Similar to (Perez et al., 1997), the nRMSE is found to increase with distance. However, the points are widely distributed around the trendlines because of the variability of the UK's solar radiation field. The range of spread is almost twice as large in winter as in summer. Large NNE / interpolation errors still occur at short distances (large nugget) due to variable cloud cover. An alternative explanation for the spreading of points in Figure 3 is the possibility of poor ground data, for example, if the stations are not adequately maintained. This is the case with most networks of automatic weather stations in all countries, although the UK Met Office is a world-leading provider of weather information.

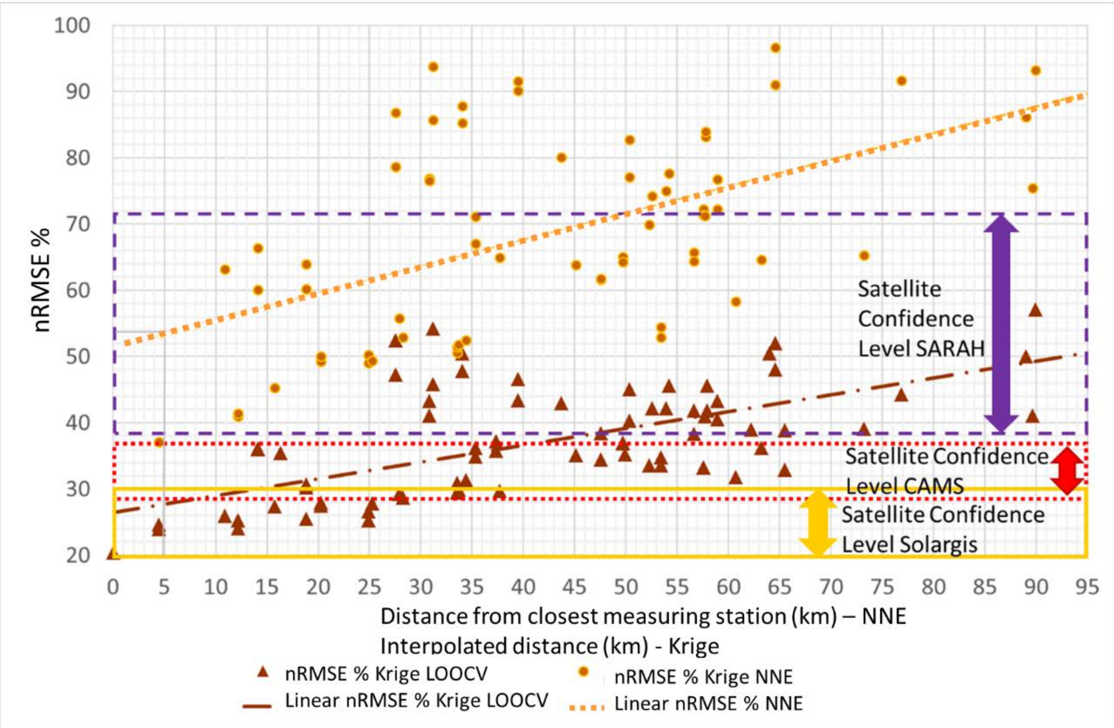


Figure 3: Satellite error relative to ground-based nearest neighbour extrapolation and kriging errors (including trends). Inter-station distances range from 600 m to 97 km.

Figure 4 is a simplified version of Figure 3, for ease of understanding. Trendlines only for nearest neighbour extrapolation nRMSE and kriging LOOCV nRMSE are marked (points removed). Satellite errors are shown as a single line for the average UK nRMSE % instead of a box for the nRMSE % range. (The satellite error average lines are placed at the halfway mark of the range boxes.) Break-even distances are labelled. The key to the labels is given in Table 1.

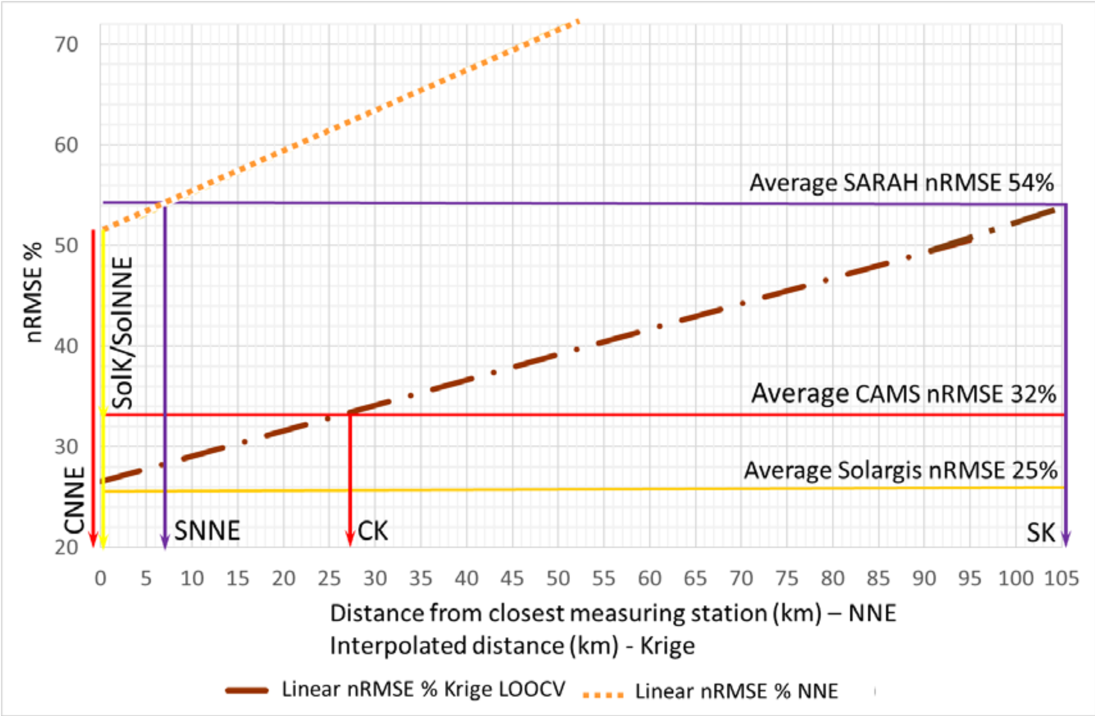


Figure 4: Satellite error relative to ground-based nearest neighbour extrapolation and kriging trends.

It may be seen that modern data is far more plentiful than that available to researchers 20 years ago. Nonetheless, the inferences are less clear. Instead of one break-even distance, there are six possibilities, one for each satellite model and NNE / kriging combination. In fact, only three break-even distances exist in reality (Table 1). The CAMS and Solargis satellite models are more accurate than NNE at all distances, on average. Solargis is also more accurate than kriging at all distances, on average. This table suggests that for most applications, NNE should not be used in the UK. Satellite data-derived data always delivers results closer to reality beyond the break-even distance.

Table 1: Break-even distances for each satellite model and NNE / interpolation combination

| Nearest Neighbour Extrapolation or Interpolation | Satellite Model | Distance in km of trendline at halfway interval of satellite confidence level box (average satellite model nRMSE) | Break-even distance label in Figure 4. |
|---|---|---|---|
| Nearest Neighbour Extrapolation | Solargis | 0 | SolNNE |
| | CAMS | 0 | CNNE |
| | SARAH | 7 | SNNE |
| Kriging | Solargis | 0 | SolK |
| | CAMS | 27 | CK |
| | SARAH | 105 | SK |

Several deductions may be observed from Figures 3 and 4. First, it is apparent that, in contrast to (Perez et al., 1997)' original work, kriging delivers a large improvement over nearest neighbour extrapolation. This is because for the current work many more ground station readings are available (80 plus as compared to 12 in 1997) and the sophisticated kriging interpolation technique is employed, rather than (Perez et al., 1997)' simpler Inverse Distance Weighting (IDW) interpolation. (IDW is necessary when data is sparse. Unlike kriging, it does not calculate probability. Interpolation can only deliver accurate results with more than 20-30 points (Huber, 2014).)

Second, satellite models generally perform better than nearest neighbour extrapolation. The exception is the SARAH model at very low distances. Third, more satellite models are available and the break-even distance is dependent on the model chosen. Fourth, the satellite models have a wide confidence level because they are extensively validated at 80 or more independent weather stations. ((Perez et al., 1997) had just one station available to them for both parameterisation and evaluation.) Fifth, the break-even distances obtained are influenced by the number of data points used, especially at the lower end of the distance scale. Finally, the break-even distances are difficult to extract accurately off the graph due to level of variation in the data.

### *3.1.2 Expansion of earlier work*

With the benefit of modern computing power, the development of the internet, increased availability of data and an extra 20 years' research into satellite modelling and kriging techniques, it is possible to expand on the original work of (Perez et al., 1997). The data from many more weather stations is available to the current researchers. In addition, MIDAS data is entirely independent of ground-based data used for parameterisation of satellite models. BSRN data is used for this purpose (BSRN, n.d.). The quantity of data also ensures the independent validation of the kriging technique because leave-one-out-cross-validation is possible. But perhaps the most significant step forward is the ability to compare NNE / kriging nRMSE with satellite errors at over 80 weather stations (Figure 5). The 1997 authors had only one weather station to calculate satellite error.

In contrast to Figures 3 and 4 which compare ground-based data to satellite confidence intervals, Figure 5 compares extrapolated and kriged data errors at each weather station to individual hourly satellite errors calculated for each same weather station. The nRMSE values are calculated as follows. At each one of the 80 weather stations the pyranometric solar irradiance value for all daylight hours in 2014 (5,116 hours) was obtained. The difference between the measured irradiance value for every hour and the value provided by each of the models (NNE, kriging and the three satellite-derived) was calculated. RMSEs were computed from this, and then the nRMSE, normalised by the mean of inputs. The average nRMSE of all the daylight hours at each weather station was calculated. The outliers in the Solargis data arise as follows. The weather station at a distance of 4km is Heathrow. This is known to be subject to reflections from passing aircraft and heat from the tarmac. The outlier at 42 km is in the Scottish Highlands where the mountains and latitude are problematic for satellite data.

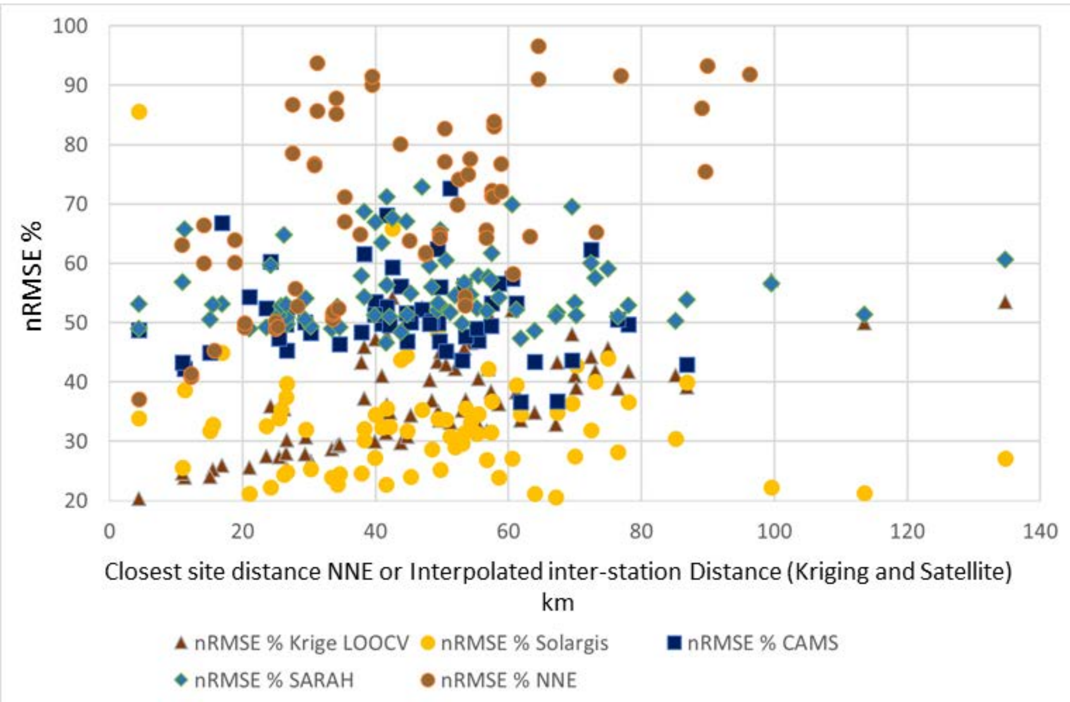


Figure 5: Satellite, NNE and kriging nRMSE at each weather station, plotted as a function of increasing inter-station distance

Figure 6 is similar to Figure 5, except that nMBE is compared to distance, rather than nRMSE. It may be seen that the CAMS product exhibits positive bias, i.e. overestimation for all stations. This has been reported several times e.g. (Copernicus, 2016). An empirical CAMS radiation bias correction is available post-2017 (Copernicus, 2017). This reduces the CAMS nMBE for UK weather stations to the same range as the other satellite models.

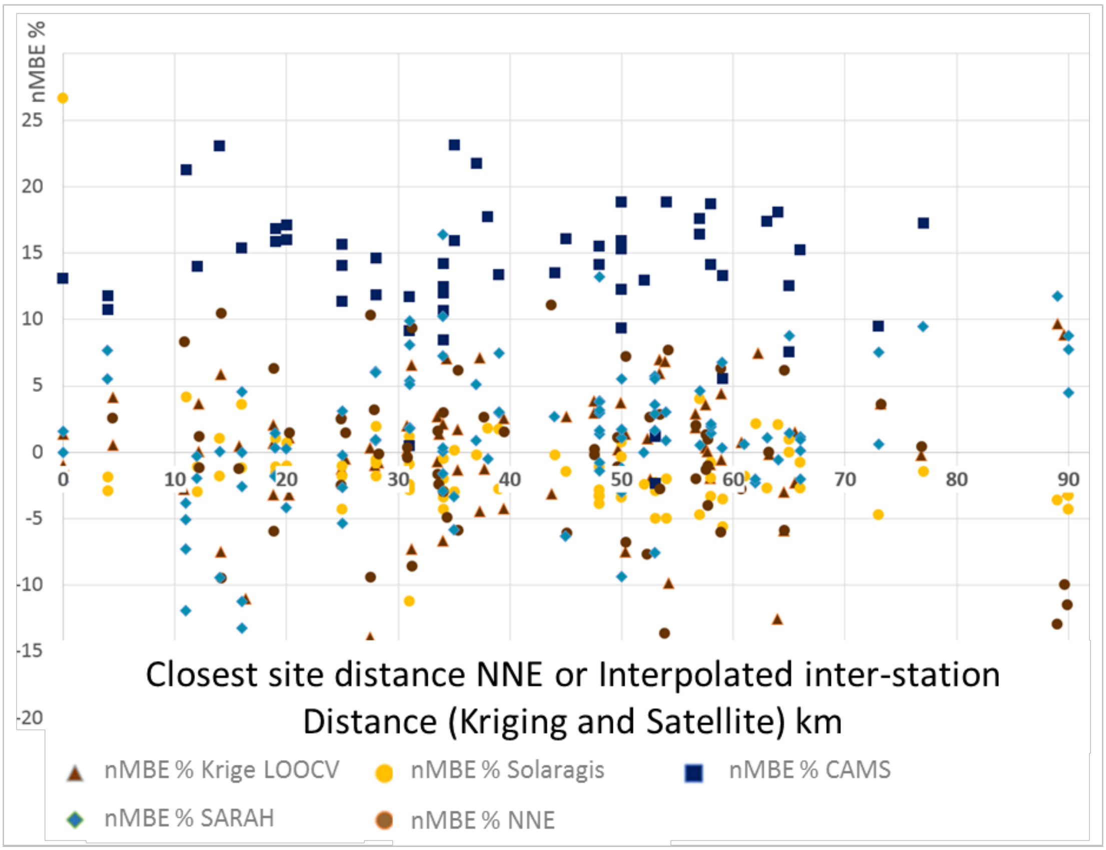


Figure 6: Satellite, NNE and kriging nMBE at each weather station, plotted as a function of increasing inter-station distance

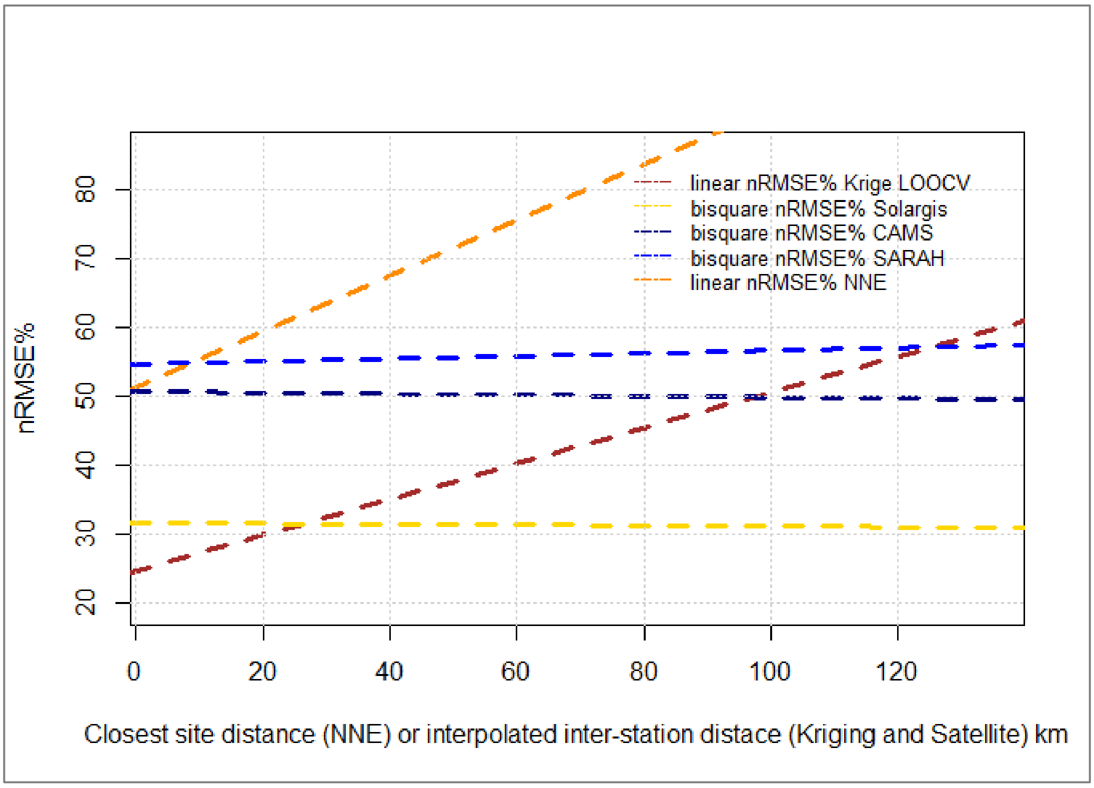


Figure 7: Trendlines of satellite, NNE and kriging nRMSE at each weather station, plotted as a function of increasing inter-station distance (km). Robust regression used to remove influence of outliers (Ripley, 2002).

Figure 7 again shows NNE / kriged and satellite nRMSE at each weather station but in the form of trendlines, for ease of interpretation. Some interesting information may be gained from Figure 7. The nRMSE of the NNE and kriging techniques rise steeply with increasing distance to weather station, whereas the nRMSE of all the satellite models have flat trends. This is as expected because the satellite data is not connected with the weather stations data. Again, kriging outperforms NNE and satellite models are more accurate than NNE. (The exception is SARAH which breaks even with NNE at 10 km.) The key difference between the initial work with satellite confidence levels (Figure 3) and nRMSE at individual weather stations (Figure 6) is the break-even distances obtained. These may be read from Figure 6 where the trendlines cross. It may be seen that kriging breaks even with the SARAH model at 125 km and with CAMS at 97 km. The furthest UK inter-station distance is 97 km and no point in the UK is more than 113 km from the sea (Haran, 2003). In the context of the UK, these distances are therefore not useful. (They could serve as guide to the applicability of SARAH and CAMS data in larger or landlocked countries.) Kriging breaks even with Solargis at 25 km. This is in agreement with other independent studies, which have shown Solargis to be the most accurate of the satellite products they tested (Ineichen, 2014, 2011).

So, of the six possible break-even distances, only one (25 km with Solargis) applies to conditions in the UK. (These conditions comprise ground data availability and impact of weather on satellite models.) Kriging of ground-measured data provides higher accuracy than the other satellite models (CAMS and SARAH) at all distances from weather stations.

Figure 8 repeats the analysis performed in Figure 7 but uses nMBE as a measure of error. All nMBE values are within the range of pyranometer error (+/- 5%), with the exception of CAMS, which has now been corrected to this range, as noted above.

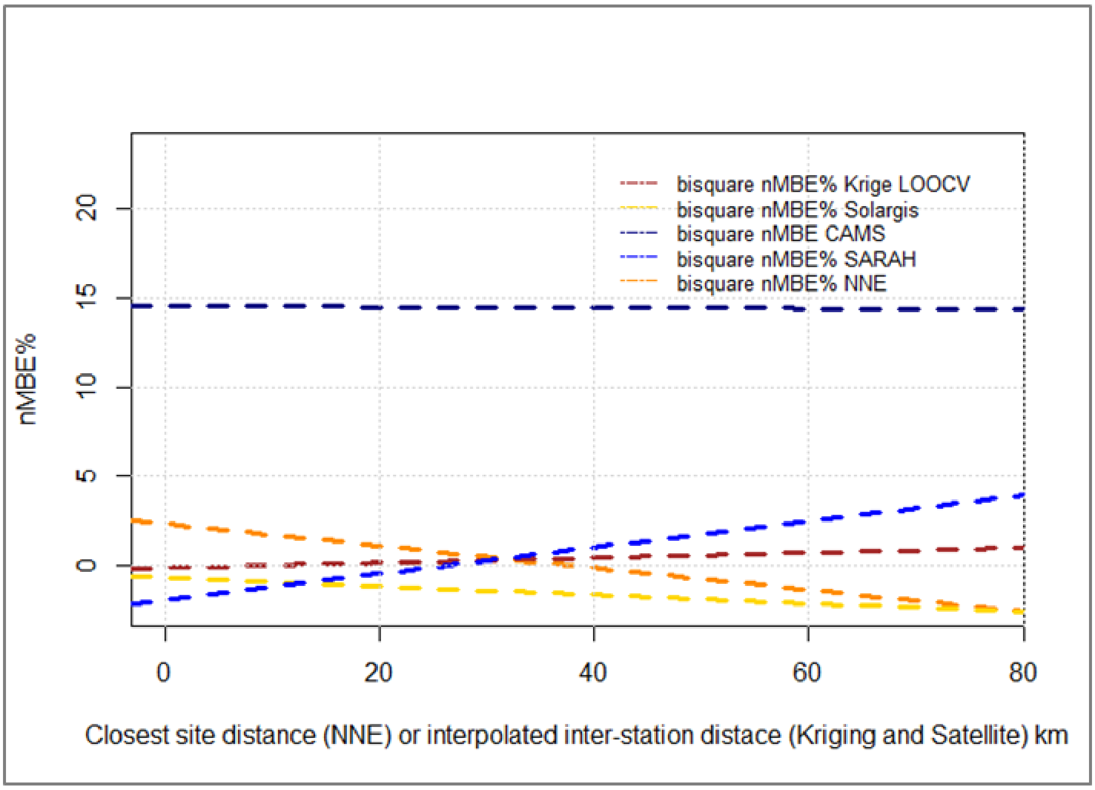


Figure 8: Trendlines of satellite, NNE and kriging nMBE at each weather station, plotted as a function of increasing inter-station distance (km). Robust regression used to remove influence of outliers (Ripley, 2002).

### *3.1.3 Application of break-even distance to the ground / satellite data decision*

Having determined a break-even distance for kriging and satellite data in the UK, it is now possible to visualise it. The appropriateness of break-even distance to the decision between use of interpolated ground-measured or satellite-derived irradiance data will also be reviewed.

Figure 9 draws the areas in the UK which are within 25 km of a weather station. The concept of break-even distance suggests that kriged data should be used inside the 25 km circles and Solargis data outside. (Note: the map would be a single colour for SARAH and CAMS because the break-even for kriging is so large the areas run into each other. Kriging outperforms SARAH and CAMS for the whole of the UK.) Figure 9 implies that kriging delivers greater accuracy in 56% of the UK and Solargis is more accurate in 44%.

It is important not to forget that the 25 km obtained is actually the *average* break even distance. The actual break-even is different for each station and it is somewhat misleading to generally apply the average.  Figure 10 indicates that for two-thirds of weather stations, Solargis is more accurate than kriging at the station. That is, in these locations, a zero break even distance should apply. Evidently, a different method of comparing kriging and Solargis errors is required.

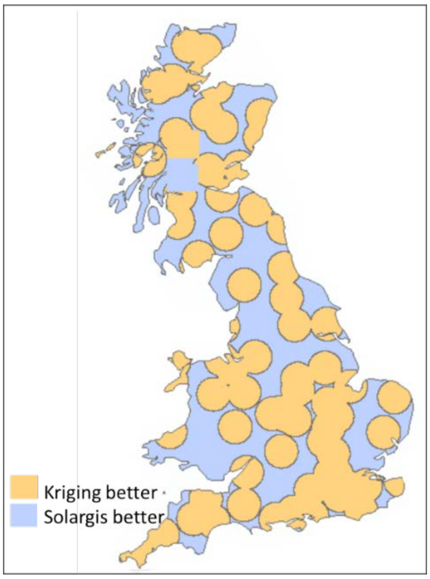


Figure 9: Map of 25 km average break-even distance between kriging and Solargis

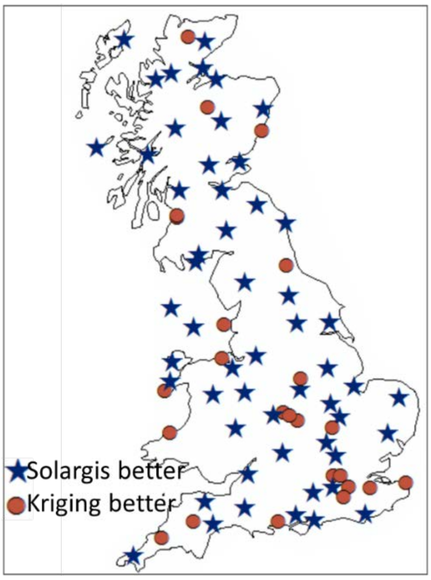


Figure 10: Map of weather stations showing whether the nRMSE of kriging or of Solargis delivers greater accuracy

Figure 11 displays the result of a two-stage process. The nRMSE of kriging and Solargis at each weather station are interpolated. These two maps are then compared. If the interpolated nRMSE of Solargis for a given pixel is less, Solargis is considered to be the best choice of irradiance data for that pixel. Likewise, if the interpolated nRMSE of kriging for a given pixel is less, kriging is considered to be the best choice of irradiance data for that pixel. This process is repeated for the nMBE in Figure 12.

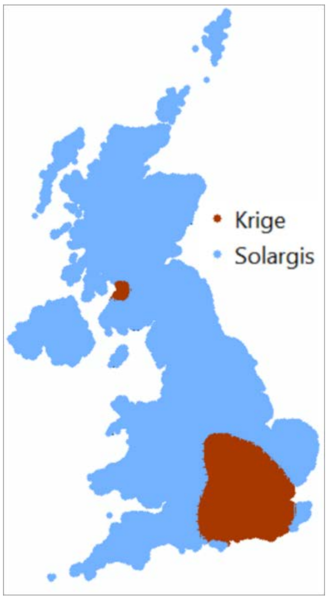


Figure 11: Areas of the UK where either kriging or Solargis offer highest accuracy, in accordance with their interpolated nRMSE

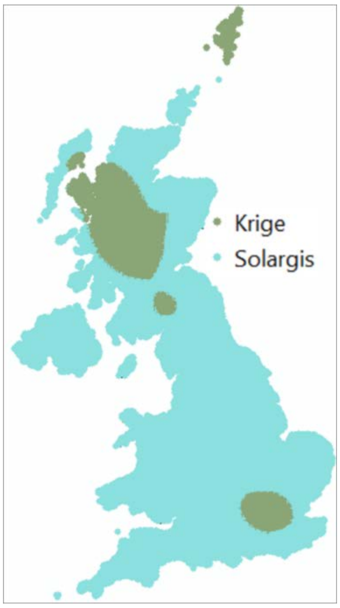


Figure 12: Areas of the UK where either kriging or Solargis offer highest accuracy, in accordance with their interpolated nMBE

It may be seen that there is a slight correlation between the interpolated errors in Figures 11 and 12 and the break-even distances in Figure 9 in the southeast of the country. Average break-even is an approximate template for selection of the irradiance data source. Figures 11 and 12 suggest that kriging is most accurate where weather stations cluster in the centre and southeast. Solargis is less accurate in the north, in terms of nMBE. This could be due to increasing latitude or due to this being a mountainous region. These factors, together with other geographic influences, are investigated in 3.2. In contrast to the break-even technique in Figure 9, interpolation of nRMSE (Figure 10) reveals that, in reality, kriging is more accurate than Solargis in just 14% of the UK.

### *3.1.4 Pyranometer Uncertainty*

Figures 5 and 7 show that Solargis is the most accurate source of irradiance data, of those tested, followed by kriging. Solargis outperforms kriging at two-thirds of weather stations (Fig. 10). Yet the mean difference between the two approaches is low: 32 kWh/m$^2$ or 4%. This section briefly investigates whether the differences are large enough to be outside the bounds of pyranometer uncertainty. (A more detailed investigation will be the subject of further research.)

Uncertainty varies with the environment and instrumentation set-up (Strobel et al., 2009). Instrumentation 1 in (Strobel et al., 2009) is equivalent to the MIDAS data sensors. The uncertainty boundaries modelled for Instrumentation 1 for Northern Europe by (Strobel et al., 2009) were applied to one year of kriged MIDAS data. It was found that kriged values and those of the Solargis satellite model only agreed within the range of pyranometer uncertainty for 17% of daylight hours in 2014. This limited correlation did not correspond to any particular irradiance values, date or time. Thus, Solargis seems genuinely the best model for the majority of the UK. Differences cannot be explained by bounds of measurement uncertainty.

## *3.2 Influence of atmospheric and topographic factors on ground or satellite irradiance data choice*

The following criteria were compared to nRMSE of the three satellite models and of the kriged data: latitude; mean sea level pressure; distance to coast; clearness index and precipitation (as representatives of cloudiness); urbanisation; cloud cover; landform; and weather station distribution. The results are summarised in Figure 23 and Tables 2 and 3.

Table 2: Influence of Distance to Weather Station, Atmospheric and Topographic Factors on Irradiance Models

| RELATIONSHIP | R SQUARED | | | |
|---|---|---|---|---|
| | Solargis | Krige | CAMS | SARAH |
| MSLP against nRMSE % ** | 0.00 | 0.52 | 0.01 | 0.45 |
| Air Mass against nRMSE % | 0.00 | 0.53 | 0.00 | 0.48 |
| Latitude against nRMSE % | 0.00 | 0.50 | 0.00 | 0.40 |
| Distance to Weather Station against nRMSE % | 0.00 | 0.47 | 0.00 | 0.00 |
| Total Cloud against nRMSE % | 0.02 | 0.38 | 0.09 | 0.46 |
| no. stations in 100 km grid sq against nRMSE % | 0.00 | 0.33 | 0.00 | 0.00 |
| Kt against nRMSE % | 0.12 | 0.20 | 0.07 | 0.46 |
| Precipitation against nRMSE % | 0.00 | 0.15 | 0.08 | 0.14 |
| Std Slope against nRMSE % | 0.05 | 0.13 | 0.05 | 0.05 |
| Relative Humidity against nRMSE % | 0.05 | 0.12 | 0.01 | 0.00 |
| Distance to Coast against nRMSE % | 0.01 | 0.06 | 0.01 | 0.01 |
| AMSL against nRMSE % * | 0.05 | 0.06 | 0.08 | 0.07 |
| Azimuth against nRMSE % | 0.03 | 0.03 | 0.03 | 0.00 |
| Hillshade against nRMSE % | 0.03 | 0.02 | 0.00 | 0.01 |
| no. stations in 45 km radius against nRMSE % | 0.00 | 0.02 | 0.00 | 0.00 |
| * Altitude above mean sea level<br>** Mean sea level pressure | | | | |

Table 3: Relationships between Geographic, Atmospheric and Topographic Factors in the UK

| RELATIONSHIP | R SQUARED |
|---|---|
| Latitude against Kt | 0.41 |
| Longitude against Kt | 0.09 |
| AMSL against Kt * | 0.06 |
| Std Slope against Kt | 0.00 |
| Latitude against Air Mass | 1.00 |
| Latitude against MSLP ** | 0.91 |
| Latitude against Total Cloud | 0.17 |
| Longitude against Total Cloud | 0.14 |
| Latitude against Relative Humidity | 0.04 |
| Latitude against no. stations in 45 km radius | 0.11 |
| Latitude against no. stations in 100 km grid sq. | 0.10 |
| Latitude against Distance to Weather Station | 0.03 |
| * Altitude above mean sea level<br>** Mean sea level pressure | |

### *3.2.1 Influence of Latitude, Coast, Precipitation, and Urbanisation*

Figure 13 illustrates the relationship between nRMSE of irradiance model and latitude.

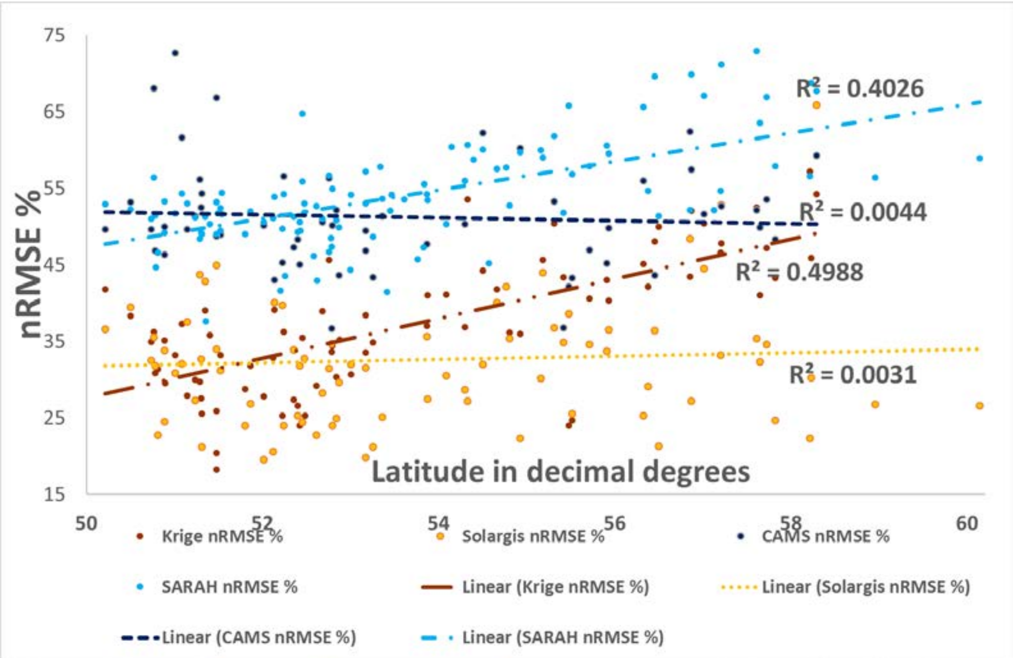


Figure 13: Trendlines of satellite and kriging nRMSE at each weather station, plotted as a function of latitude

It may be seen that the performance of SARAH and kriging vary with latitude, CAMS and Solargis much less so. Latitude is known to have a negative effect on satellite models, due to parallax. The more sophisticated CAMS and Solargis models handle this better. The apparent influence of latitude on the kriging model is probably a result of the north of the UK being more mountainous and having fewer weather stations (see sections 3.2.2 and 3.2.3). These factors cannot be separated in the UK. The statistical significance of decrease in number of weather stations with latitude (Table 3) is slender. Distribution of stations can be explained by population density and accessibility (Kilibarda et al., 2015), which in turn are influenced by terrain. In the UK these tend to decrease northwards but the exceptions are the cities of Glasgow and Edinburgh in southern Scotland. Figure 14 compares weather station distribution in terms of count per Ordnance Survey 100 km grid square with major cities and the motorway network.

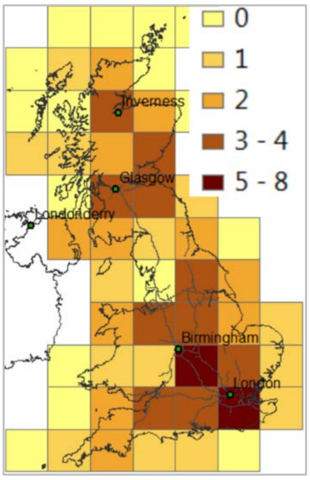


Figure 14: Count of weather stations per Ordnance Survey 100 km grid square

Figure 15 plots the relationship between nMBE of irradiance model and latitude.

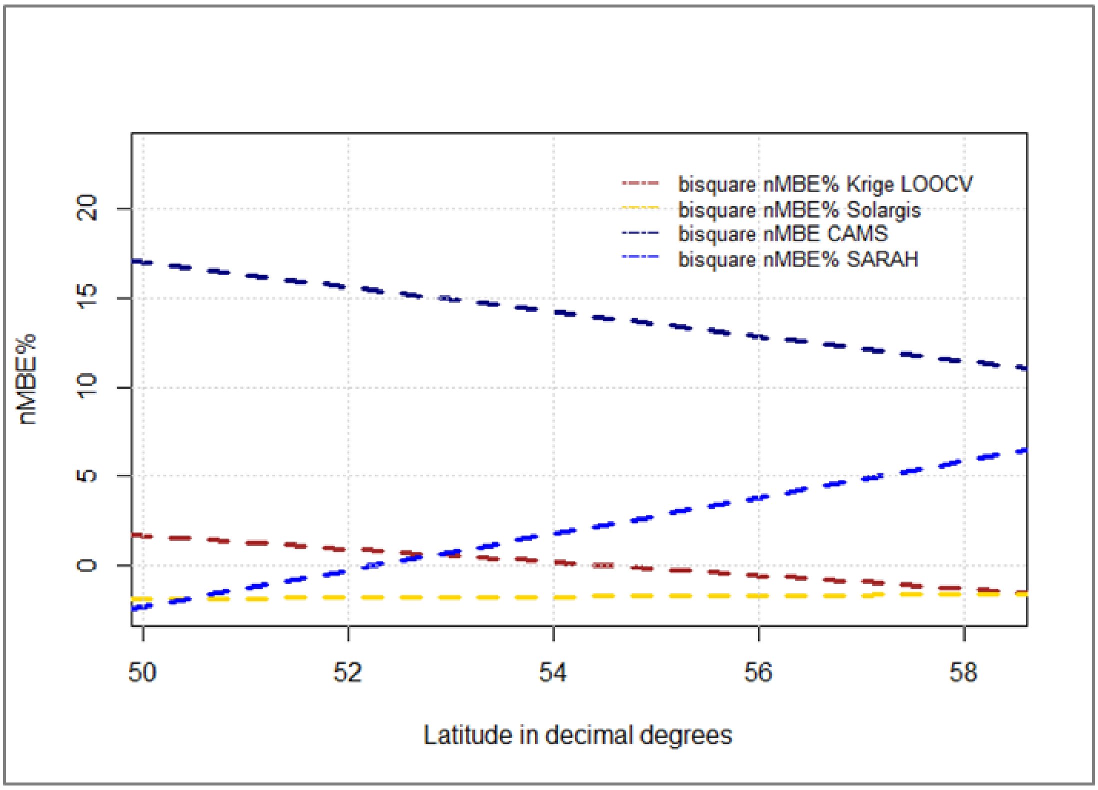


Figure 15: Trendlines of satellite and kriging nMBE at each weather station, plotted as a function of latitude. Robust regression used to remove influence of outliers (Ripley, 2002)

With the exception of CAMS (now corrected), the nMBE of all irradiance models is within pyranometer error. The unanticipated phenomenon of CAMS nMBE decreasing northwards in the UK is in agreement with the map produced by (Wald, 2017).

Higher latitudes may also be associated with increased cloud cover or cloud variability (Wetherald and Manabe, 1986). In the UK, this was indeed found to be the case. A statistical test showed an association between clearness index, Kt, (hourly GHI as a fraction of extraterrestrial irradiance), and latitude ($R^2$ = 0.41) A comparison of nRMSE with Kt found that all models show increased accuracy with clearer skies (Figure 16). SARAH shows a greater increase in accuracy with clearer skies than the other models.

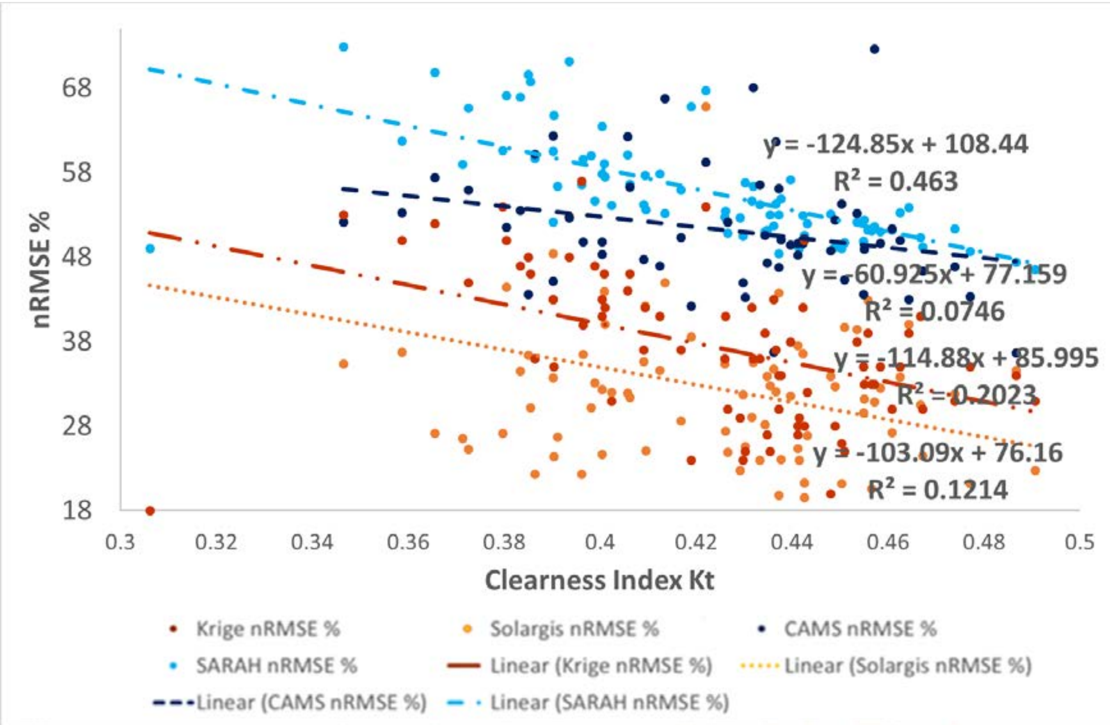


Figure 16: Average hourly nRMSE % per site for 2014 as a function of average hourly clearness index, Kt per site

Another factor linked to latitude in the UK is atmospheric pressure (mean sea level pressure) ($R^2$ = 0.91). Low pressure areas, formed between the tropical and polar air masses in the Atlantic, approach the UK from southwest to northeast, due to the west to east direction of the upper Polar Front Jet Stream. The correlation between nRMSE of irradiance model and mean sea level pressure is shown in Figure 17. SARAH and kriging both show some negative correlation with pressure. That is, the model errors decrease as the pressure increases. High pressure reduces the formation of cloud, so these two models are performing better under stable, clear conditions. This has already been seen with the clearness index. MSLP has little influence on CAMS and Solargis nRMSE because these models are more resilient in the presence of cloud.

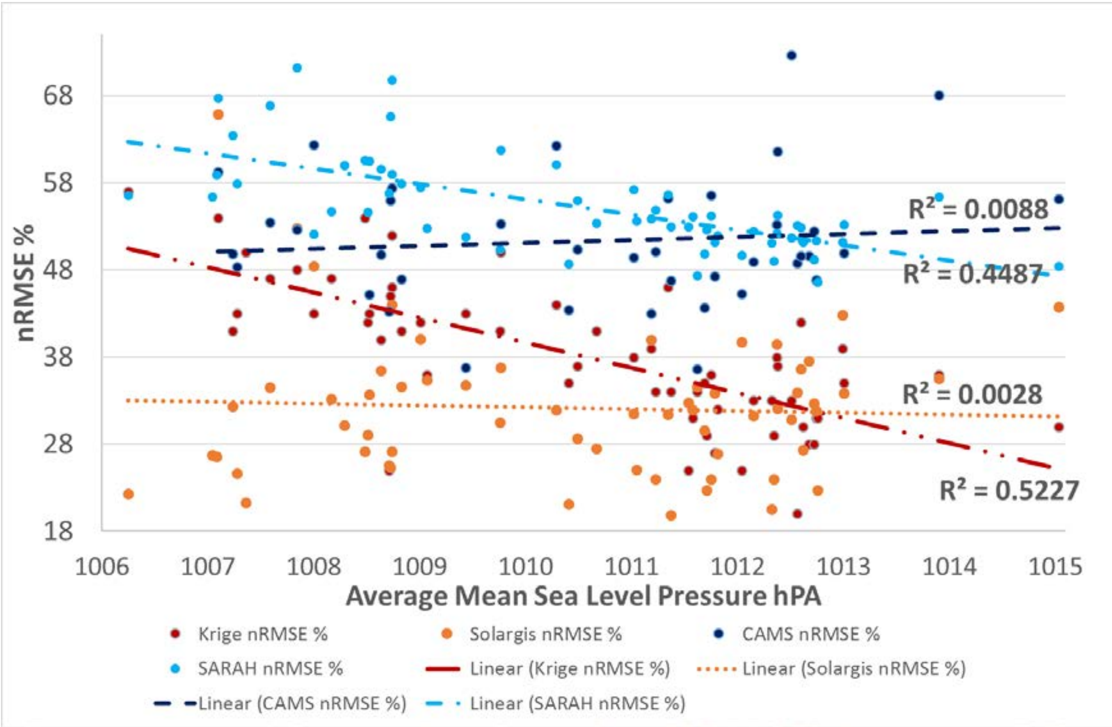


Figure 17: Average hourly nRMSE % per site for 2014 as a function of average Mean Sea Level Pressure per site

Plots of nRMSE % at weather station against distance to coast delivered flat trends in all cases. Proximity to coast is known to impact satellite models. The UK is entirely coastal in terms of coastal cloud formation and maritime aerosols, so no deductions are possible in this case. Definitions of 'coastal' vary being between 80 and 100 km of shoreline (NOAA Office for Coastal Management, 2016; Small and Nicholls, 2003). The furthest point from tidal water in the UK is only 72 km away (Haran, 2003).

A weak association between precipitation and modelled irradiance values was detected. The weakness of the association is due the fact that cloud cover in the UK frequently does not result in rain. The connection between relative humidity and irradiance model errors was likewise found to be slight. Aerosols must also be present for clouds to form (Appendix C). Kriging does not account for cloudiness at all, whilst Solargis has several innovations which improve its performance (GeoModelSolar, 2012).

An attempt to correlate RMSEs of modelled irradiances with rural urban classification (DEFRA, 2013) proved inconclusive. This is probably due to the fact that no UK weather station is more than 32 km from an urban area.

### *3.2.2 Cloud Cover*

As noted in Section 3.2.1, higher latitudes may be subject to persistent cloudiness and the frequent appearance of broken clouds. Hourly cloud cover and cloud type (measured in oktas) from (UK Met Office, 2006) were analysed. The statistical relationship between average hourly cloud cover and UK latitude is not strong ($R^2$ = 0.17, Table 3). The cloud cover to longitude association is even less convincing ($R^2$ = 0.04). This is probably because broken cloud (5-6 oktas) prevails across the majority of the country 90% of the year. However, interpolation of average hourly cloud cover for 2014 from 286 weather stations (Figure 18) illustrates a visual link between cloud cover, latitude and longitude. Cloud amount increases from the southeast to the northwest. Comparison of Figure 18 with the nRMSE % distributions of the satellite and kriging algorithms in Figures 20 and 21 also suggests causality between cloud cover and modelled irradiance error. This is especially clear in the cases of kriging and SARAH ($R^2$ = 0.38 and 0.46 respectively, Table 2).


Figure 18: Map of interpolated average hourly cloud cover (2014)

A study of latitude and cloud type indicates a stronger relationship between medium cloud and latitude than either low or high cloud (Table 4). The way the different clouds form may explain this observation. Low clouds e.g. cumulus and stratocumulus clouds form over land when the air is heated by the ground and rises. The air temperature drops and water vapour condenses. This effect will occur nationwide. Low stratus cloud results from orographic forcing, with presence of British mountains being linked to latitude. Mid-atlantic depressions which track across the UK from southwest to northeast generate the following sequence of cloud cover as they pass through: high, then medium and finally low. The cloud composition on the weather fronts differs according to air stability and atmospheric temperature gradients (AQA, n.d.).

Table 4: R Squared value for relationship between cloud types and latitude

| RELATIONSHIP | R Squared |
|---|---|
| Latitude against Low Cloud | 0.06 |
| Latitude against Medium Cloud | 0.13 |
| Latitude again High Cloud | 0.02 |

Comparison of cloud type and solar irradiance models reveals that all models are influenced by low cloud to approximately the same extent (Table 5). Low cloud provides the largest average contribution to overall cloud cover in the UK (average low cloud = 5 oktas, average medium cloud = 2 oktas, average high cloud = 1 okta.) Solargis, kriging and SARAH are influenced by low cloud rather than by medium or high cloud. Low level stratus cloud can cover most of the sky, medium level altostratus allows more penetration of irradiance, whereas high level cirrus is wispy (UCAR, 2012). CAMS shows a different pattern of cloud type influence, possibly due to its more frequent aerosol optical depth input.

Table 5: R Squared value for relationship between cloud types and modelled irradiance errors

| RELATIONSHIP | Solargis | Krige | CAMS | SARAH |
|---|---|---|---|---|
| Total Cloud against nRMSE % | 0.02 | 0.38 | 0.09 | 0.46 |
| Low Cloud against nRMSE % | 0.27 | 0.31 | 0.36 | 0.3 |
| Medium Cloud against nRMSE % | 0 | 0 | 0.66 | 0.12 |
| High Cloud against nRMSE % | 0 | 0 | 0.54 | 0 |

### *3.2.3 Landform*

Typical landforms include hills, mountains and plains. Landforms may be categorised by several physical attributes; the ones of interest to this research are elevation (altitude above mean sea level - AMSL) and change of elevation (or lack of). Change of elevation is associated with slope, aspect and prominence (height above lowest contour line) i.e. terrain ruggedness. AMSL in the UK is low, compared to most other European countries. Even so, there are over 3,000 mountains in the U.K. with a minimum height of 2,000 feet (610 m), There are also more than 16,000 "tumps" with a prominence of 30 m (Jackson et al., 2017).

A plot of nRMSE against AMSL revealed a weak relationship (slope of 0.02) for all models. Therefore terrain ruggedness was investigated. There are several ways to quantify topographic ruggedness (Cooley, 2016). Here standard deviation of slope is used because it performs well at all scales and is conceptually simple (Grohmann et al., 2011). The slope data used was the Shuttle Radar Topography Mission (SRTM) 90 m cell size digital elevation grid (Pope, 2017). Figure 19 indicates that all models are disadvantaged by complex terrain. Kriging is more impacted than the satellite models because it does not interpolate in the z plane. This may also be seen in Table 6 which averages nRMSE % inside and outside of Less Favoured Areas (LFA). These are EU-defined mountainous and hill farming areas (EU, 2013).

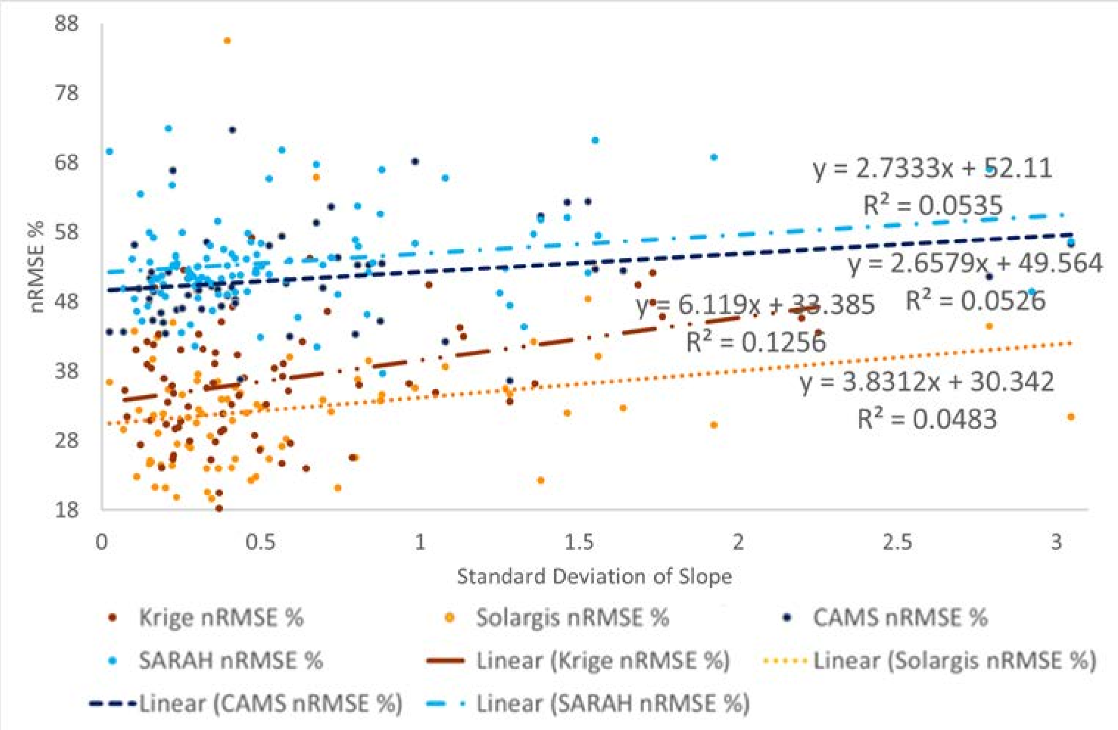


Figure 19: Trendlines of satellite and kriging nRMSE at each weather station, plotted as a function of Standard Deviation of Slope

Table 6: Average nRMSE % inside and outside of Less Favoured (hill and mountain) Areas.

| | Average nRMSE % in LFA | Average nRMSE % outside of LFA |
|---|---|---|
| Krige | 44 | 34 |
| Solargis | 34 | 32 |
| CAMS | 54 | 50 |
| SARAH | 58 | 53 |

An investigation was carried to out establish the relationship between standard deviation of slope and the clearness index. In theory, cloudiness should increase with terrain complexity due to orographic forcing. In fact, the resultant graph based on UK data showed no link between these variables (flat trend). A Kt/elevation plot was also non-conclusive. The influence of terrain ruggedness on solar irradiance models in the UK must be due to another associated factor. Hillshade was generated using ArcGIS software (ESRI, 2014). All the models show a non-significant reduction in error as shadowing decreases. When azimuth was studied, the kriging model nRMSE displayed a non-significant relationship. None of the satellite models showed any correlation to azimuth. The connection between terrain and irradiance appears to be complex and not easily explained with hourly data (Tables 2 and 3).

Figure 20 illustrates the nRMSE % for each modelled irradiance value at each weather station in interpolated format (for ease of interpretation). The nRMSE maps are compared to terrain ruggedness in the form of a map of standard deviation of slope. It can be seen that kriging and SARAH have high errors in areas of complex terrain (mountains) and lower errors in flat regions, whereas Solargis is robust against topographic features.

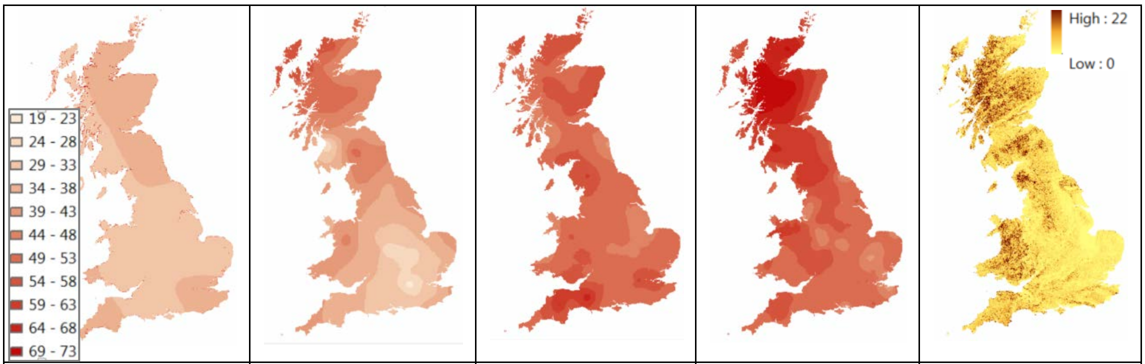


| | | | | |
|---|---|---|---|---|
| Solargis | Kriging | CAMS | SARAH | Std Dev of Slope |
| (a) | (b) | (c) | (d) | (e) |

Figure 20: Maps of interpolated nRMSE % of satellite and kriging algorithms compared to map of Standard Deviation of Slope

Figure 21 investigates the degree to which errors at adjacent weather stations are similar for each irradiance model. Anselin Local Moran's I index is calculated, mapped and compared to the map of terrain ruggedness. Anselin Local Moran's I allows identification of spatial groups of objects with features of the same magnitude (Anselin, 2010; Renard, 2017). This index enables statistically significant groups with high (HH) and low (LL) error values to be distinguished. Again, in the cases of kriging and SARAH, a link with terrain ruggedness is detected.

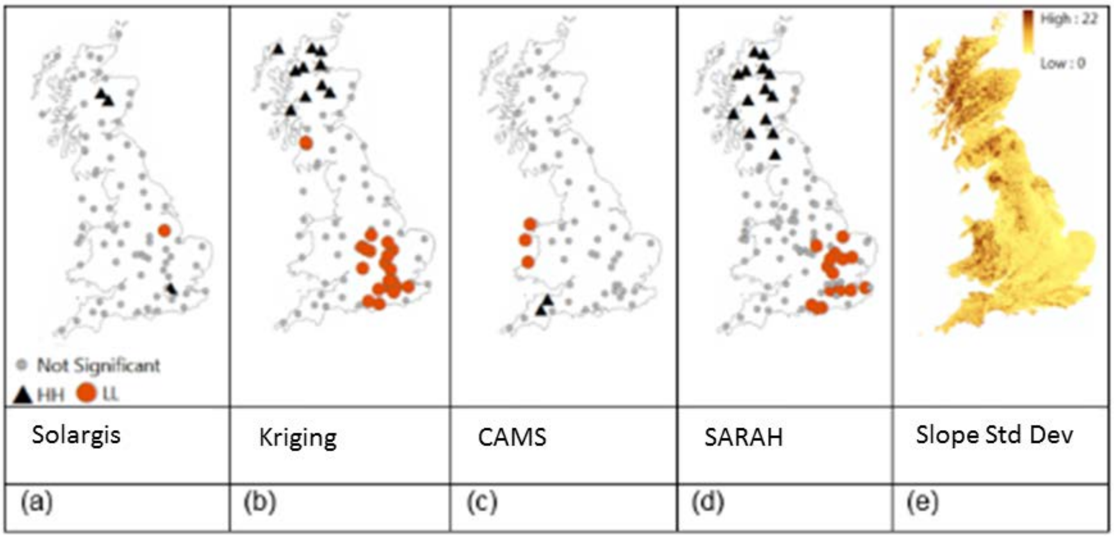

Figure 21: Maps of Anselin Local Moran's I index at each weather station for satellite and kriging algorithms compared to map of Standard Deviation of Slope

There is another way in which terrain may influence solar irradiance. As altitude above mean sea level (AMSL) increases, the atmosphere becomes thinner (less pressure). Thus the total amount of water vapour the atmosphere can potentially hold is decreased and more solar irradiance penetrates at higher altitudes. However, increases in daily totals of global irradiance with altitude have been reported as 6-10% per 1000 m (Blumthaler et al, 1997). The difference in ground height between the highest and lowest UK weather station is only 360 m. Therefore, altitude effect could only account for a small percentage of changes in the UK solar irradiance data.

Absolute humidity (mass of water vapour in a unit volume of air kg/m3) was calculated from MIDAS weather station values for relative humidity and temperature using the NOAA Moisture Calculator (Padfield, 2013). The trend for water vapour to decrease with rising elevation in the UK is slender ($R^2$ = 0.01). When absolute humidity is compared to irradiance model errors, no relationship was found for any of the satellite models (flat trends). This suggests that they all address altitude effects well. In the case of kriging, nRMSE decreases with increasing water vapour content ($R^2$ = 0.5), in contrast to expectations. Also, plotting average hourly global horizontal irradiance against weather station AMSL gave a slight anticorrelation ($R^2$ = 0.02). These last two statistics suggest that, in upland areas in the UK, the effect of irradiance increasing with altitude is outweighed by cloud formation associated with rising terrain.

### *3.2.4 Weather Station Distribution*

Maps of interpolated nRMSE for the irradiance values from the kriging algorithm were generated, with colour ramps optimised to the kriging error values (Figure 22). These were overlaid with the location of weather stations. There is a clear visual link between clustering of weather stations and low errors. (There is, of course, no relationship between clustering of MIDAS stations and any of the satellite models because these do not utilise MIDAS data.)

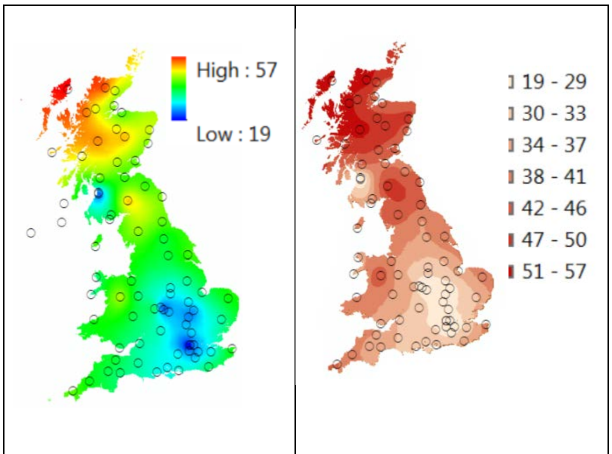


| Stretched colour ramp | Classified colour ramp |
|---|---|
| (a) | (b) |

Figure 22: Maps of interpolated nRMSE % of kriging algorithms overlaid with weather station location

Several techniques were experimented with to ascertain how to quantify this link mathematically. Weather station density and neighbour count in distance band gave the simplest and most reliable results (Table 7).

Table 7: Results of techniques quantifying weather station clustering

| Weather Station Density | | Neighbour Count in Distance Band | |
|---|---|---|---|
| Area | No. weather stations per 100 x 100 km grid square (10,000 $km^2$) | No. neighbours within 100 km radius of each weather station | No. neighbours within 45 km radius of each weather station |
| All UK | 3 | 2 (+ station itself = total of 3 in circular area) | n/a |
| Areas where kriging performs best (< 30 % nRMSE) | 6 | n/a | 2 (+ station itself = total of 3 in circular area) |

Looking at Figures 11 and 14, it is evident that kriging outperforms Solargis where there are at least 6 weather stations per 10,000 $km^2$ grid square. Kriging outperforms CAMS and SARAH throughout the UK i.e. where there is a weather station density of at least 3 weather stations per 10,000 $km^2$ grid square. Three per 10,000 $km^2$ grid square is possibly achievable for many national meteorological organisations, but perhaps not more than this. It is surmised that this is the lowest weather station density for interpolation to surpass satellite model accuracy. PVGIS Classic/Original PVGIS/PVGIS-3 (JRC, 2012a), computed from interpolation of data from 566 ground meteorological stations throughout the European Subcontinent, has a new version, PVGIS-4/PVGIS-CMSAF. PVGIS Classic has 2 weather stations per 10,000 $km^2$ grid square. The new version is based on calculations from CMSAF satellite images and its authors are convinced it is an improvement on PVGIS Classic in most places (JRC, 2012b).

### *3.2.5 Major topographic influences on ground or satellite irradiance data choice*

These are presented in Table 2 and Figure 23.

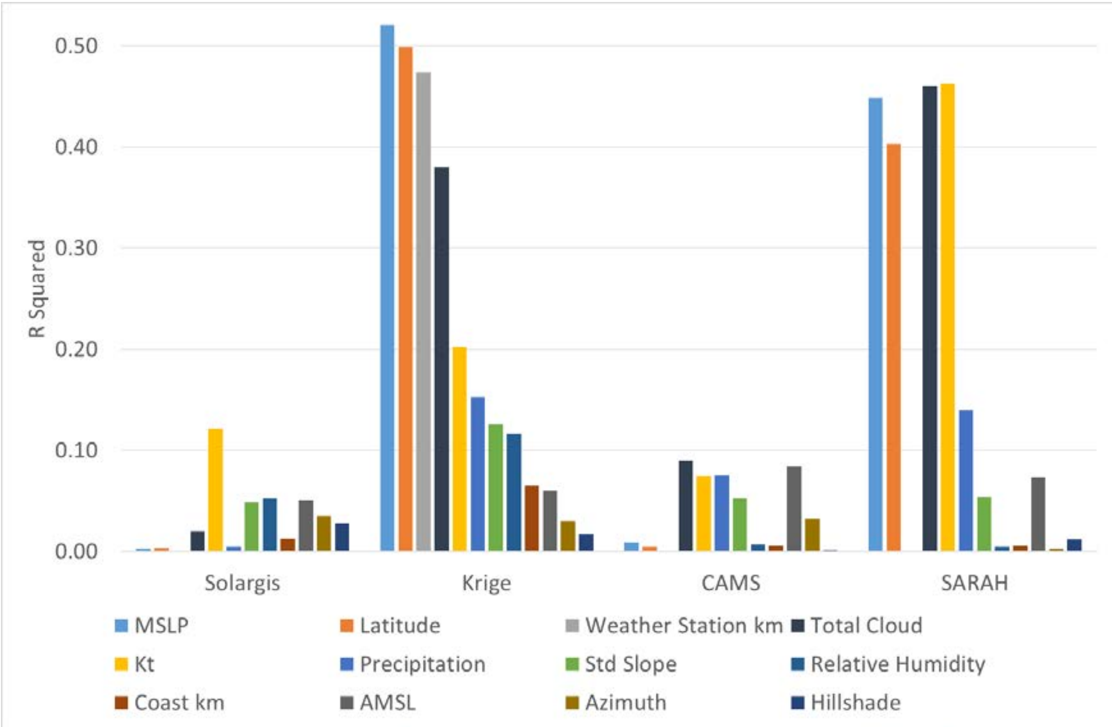


Figure 23: Influence of Distance to Weather Station, Atmospheric and Topographic Factors on Irradiance Models

Reviewing sections 3.2.1 to 3.2.3 (with Table 2 and Figure 23), it is apparent that the SARAH model is affected by factors associated with latitude and cloudiness (MSLP, Total Cloud Cover and Kt), and to a lesser extent by terrain. Kriging accuracy is determined by: factors associated with latitude and cloudiness; weather station clustering; less strongly by terrain. In the cases of Solargis and CAMS, none of the factors tested heavily influence error distributions (Figure 23).

Thus, when deciding between ground-measured and satellite-derived irradiance values, terrain, latitudinal factors and weather station clustering are the factors which matter. Some satellite models treat problems due to latitude and terrain more successfully than others. The SARAH model is less accurate than the CAMS and Solargis models. SARAH uses long-term monthly modelled averages for atmospheric input data (Appendix C). These long-term monthly aerosol averages smooth daily fluctuations. CAMS and Solargis employ satellite-derived 3-hourly and daily calculated values respectively. Short-term calculated values have an additional advantage over satellite data in that any missing data is filled in (Cebecauer et al., 2011), suggesting that Solargis may have the most accurate atmospheric inputs.

# 4. Conclusion

This research delivers a national assessment of which data source is most accurate for production of site specific hourly irradiance data: satellite-derived values or ground-based measurements. Furthermore, it explores the atmospheric and geographic conditions under which each solar radiation resource delivers the most accurate results. The models tested may be listed in decreasing order of accuracy as follows: Solargis, kriging of ground measurements, CAMS, SARAH and nearest neighbour extrapolation of ground measurements. The exception is where there are at least 6 weather stations per 10,000 $km^2$ grid square. In these circumstances, kriging outperforms Solargis.

It was noted that nearest neighbour extrapolation does not deliver accurate results. Choice of satellite model is influential. The decision is not between satellite-derived and ground-based data, but between *which* satellite model and *interpolation* of ground measurements.

All the irradiance models evaluated were affected by landform, SARAH and kriging also by latitude. In the UK these factors cannot be separated since topographic ruggedness increases with latitude. Generally, it is not the case that some models perform better under certain terrestrial circumstances than others. Solargis has lower errors over the entire UK than CAMS, which is in turn is more accurate nationwide than SARAH. Satellite model accuracy appears to be related to time resolution of atmospheric input data.

Regarding the satellite/interpolated values decision, break-even distance provided guidance, but it can be enhanced. Rather than distance from weather station, the number of neighbours in distance band or number of weather stations per 100 x 100 km grid square (weather station clustering/density), are more effective rules. These demonstrate a closer representation of reality. Of the datasets tested in this paper, kriging is more accurate than SARAH and CAMS where there are at least 3 weather stations per 100 x 100 km grid square or 2 neighbours in a 100 km distance band of each weather station. Kriging is more accurate than Solargis where there are at least 6 weather stations per 100 x 100 km grid square or 2 neighbours in a 45 km distance band of each weather station. Weather station density is key. It is conjectured that in countries with less variable climates and landscapes e.g. flat desert, greater interpolation accuracy may be achieved with fewer ground measurements. For instance, research using data from ten meteorological stations located in the south and centre of Tunisia (Loghmari and Timoumi, 2017) has found solar irradiance data may be accurately extrapolated for distances of 65 – 129 km.

Influence of station network density has been recognised in studies of rainfall and temperature (Hofstra et al., 2010; Yang et al., 2016) but not previously been investigated for solar irradiance.

The most recent developments in satellite-based modelling of solar irradiance combine long-term satellite values with short-term high-accuracy ground measurements. This technique of site adaptation enables the production of enhanced historical data for new sites e.g. solar farms with measurement facilities. Validation against independent data has shown impressive improvements in error values (Cebecauer and Suri, 2016; Polo et al., 2016; Ruiz-Arias, J.A., Quesada-Ruiz, S., Fernández, E.F., Gueymard, 2015).

Satellite data itself will also improve with the launch of the Meteosat Third Generation series from 2021 onwards. The new satellites will provide images at high spatial resolutions, from 2 km to 0.5 km, as well as higher quality aerosol data. The ability of satellite irradiance algorithms to handle broken cloud will be enhanced and more accurate data for the radiative transfer equations will become available. Thus, in future, it may be possible that satellite-derived irradiance values will match or exceed the accuracy of data interpolated from even the highest density station networks.

## Acknowledgements

The authors would like to thank Jose A Ruiz-Arias for his advice which greatly improved the manuscript. We are also grateful to the Solargis team for supplying data.

This work has been conducted as part of the research project ‘Joint UK-India Clean Energy Centre (JUICE)’ which is funded by the RCUK's Energy Programme (contract no: EP/P003605/1). The projects funders were not directly involved in the writing of this article.

## References

Amillo, A., Huld, T., Müller, R., 2014. A New Database of Global and Direct Solar Radiation Using the Eastern Meteosat Satellite, Models and Validation. Remote Sens. 6, 8165–8189. https://doi.org/10.3390/rs6098165

Anselin, L., 2010. Local Indicators of Spatial Association-LISA. Geogr. Anal. 27, 93–115. https://doi.org/10.1111/j.1538-4632.1995.tb00338.x

AQA, n.d. Origin and nature of depressions. URL http://www.coolgeography.co.uk/A-level/AQA/Year%2013/Weather%20and%20climate/British%20Isles/British-Depressions.htm (accessed 16/02/2018)

Blumthaler, M., Ambach,W. and Ellinger, R. 1997. Increase in solar UV radiation with altitude. Journal of Photochemistry and Photobiology B: Biology, 39, 2, 130-134. URL https://doi.org/10.1016/S1011-1344(96)00018-8 (accessed 22/02/2018)

BSRN, n.d. World Radiation Monitoring Center - Baseline Surface Radiation network [WWW Document]. URL http://bsrn.awi.de/ (accessed 21/06/2017).

Cebecauer, T., Marcel, Š., Gueymard, C.A., 2010. Uncertainty Sources in Satellite-Derived Direct Normal Irradiance: How Can Prediction Accuracy Be Improved Globally? Proc. SolarPACES Conf. 20–23. URL https://www.researchgate.net/profile/Chris_Gueymard/publication/228481494_Uncertainty_sources_in_satellite-derived_direct_normal_irradiance_how_can_prediction_accuracy_be_improved_globally/links/0deec517ff684d35ec000000/Uncertainty-sources-in-satellite-derived-direct-normal-irradiance-how-can-prediction-accuracy-be-improved-globally.pdf (accessed 02/02/2018)

Cebecauer, T., Suri, M., 2016. Site-adaptation of satellite-based DNI and GHI time series: Overview and SolarGIS approach Evaluation of parasitic consumption for a CSP plant Site-adaptation of Satellite-based DNI and GHI Time Series: Overview and SolarGIS Approach. AIP Conf. Proc. AIP Conf. Proc. AIP Conf. Proc. 17341, 150002–150005. https://doi.org/10.1063/1.4949234

Cebecauer, T., Suri, M., Perez, R., 2010. High performance MSG satellite model for operational solar energy applications, in: Proc. Solar 2010. ASES Annual Conference. Phoenix, AZ. URL http://proceedings.ases.org/wp-content/uploads/2014/02/2010-086small.pdf (accessed 02/02/2018)

Cooley, S., 2016. Terrain Roughness – 13 Ways [WWW Document]. GIS 4 Geomorphol. URL http://gis4geomorphology.com/roughness-topographic-position/ (accessed 19/07/2017).

Copernicus Atmospheric Monitoring Service, 2016. Standard Validation Report of Solar Radiation Products Issue #5 J-F-M 2014, ECMWF Copernicus. URL https://atmosphere.copernicus.eu/sites/default/files/FileRepository/Resources/Validation-reports/Solar_radiation/CAMS72_2015SC1_72.1-2_D1-2014Q1_201606.pdf (accessed 06/02/2018)

Copernicus Atmospheric Monitoring Service, 2017. Proposal for the inclusion of a bias correction in the CAMS Radiation Service Proposed by Armines to Transvalor, ECMWF Copernicus. URL http://www.soda-pro.com/documents/10157/326332/CAMS72_2015SC2_note_201707_acceptance_bias_correction_v1.pdf/1e3fa565-b616-4ded-9bcd-05841b3ba3ac (accessed 06/02/2018)

DEFRA, 2013. 2011 Rural Urban Classification [WWW Document]. Off. Stat. URL https://www.gov.uk/government/statistics/2011-rural-urban-classification (accessed 02/02/2018)

ESRI, 2014. ArcGIS Desktop: Release 10.3. URL http://desktop.arcgis.com/en/arcmap/10.3/get-started/license-manager-guide/supported-software-products.htm (accessed 02/02/2018)

EU, 2013. EU review of less favoured areas - Council Directive 75/268/EEC [WWW Document]. URL https://www.gov.uk/government/consultations/eu-review-of-less-favoured-areas (accessed 19/07/2017).

GeoModelSolar, 2012. SolarGIS Database version 1.8 satellite-derived solar radiation and meteorological data. Bratislava. URL https://solargis.info/ (accessed 02/02/2018)

Grohmann, C.H., Smith, M.J., Riccomini, C., 2011. Multiscale Analysis of Topographic Surface Roughness in the Midland Valley, Scotland. IEEE Trans. Geosci. Remote Sens. 49, 1200–1213. https://doi.org/10.1109/TGRS.2010.2053546

Hall, J., Hall, J., 2010. Solar Data Warehouse - Evaluating the Accuracy of Solar Radiation Data Sources. URL http://www.solardatawarehouse.com/whitepaper.pdf (accessed 02/02/2018)

Haran, B., 2003. The farm furthest from the sea. BBC News. URL http://news.bbc.co.uk/1/hi/england/derbyshire/3090539.stm (accessed 02/02/2018)

Hofstra, N., New, M., McSweeney, C., 2010. The influence of interpolation and station network density on the distributions and trends of climate variables in gridded daily data. Clim. Dyn. 35, 841–858. https://doi.org/10.1007/s00382-009-0698-1

Huber, W., 2014. arcgis 10.1 - Minimum number of samples for kriging interpolation -

Geographic Information Systems Stack Exchange [WWW Document]. StackExchange. URL https://gis.stackexchange.com/questions/50584/minimum-number-of-samples-for-kriging-interpolation (accessed 19/07/2017).

Ineichen, P., 2014. Long term satellite global , beam and diffuse irradiance validation. Energy Procedia 48, 1586–1596. https://doi.org/10.1016/j.egypro.2014.02.179

Ineichen, P., 2011. Five satellite products deriving beam and global irradiance validation on data from 23 ground stations. (333.7-333.9) Geneva. URL https://archive-ouverte.unige.ch/unige:23669 (accessed 02/02/2018)

Jackson, G., Crocker, C., Barnard, J., Edwards, S., Gradwell, G., Jackson, M., Bloomer, J., Marshall, D., 2017. The Database of British and Irish Hills v15.5 [WWW Document]. URL http://www.hills-database.co.uk (accessed 19/07/2017).

Journée, M., Bertrand, C., 2011. Quality control of solar radiation data within the RMIB solar measurements network. Sol. Energy 85, 72–86. https://doi.org/10.1016/j.solener.2010.10.021

JRC, 2012a. PVGIS [WWW Document]. URL http://re.jrc.ec.europa.eu/pvgis/apps4/pvest.php?lang=en&map=europe (accessed 16/06/2017).

JRC, 2012b. PVGIS [WWW Document]. URL http://re.jrc.ec.europa.eu/pvgis/apps4/databasehelp_en.html (accessed 02/01/2017).

Kilibarda, M., Tadic, M.P., Hengl, T., Bajat, B., 2015. Global geographic and feature space coverage of temperature data in the context of spatio-temporal interpolation. Spat. Stat. 14, 22–38. URL https://www.sciencedirect.com/science/article/pii/S2211675315000299 (accessed 02/02/2018)

Loghmari, I, and Timoumi, Y., 2018. Performance comparison of two global solar radiation models for spatial interpolation purposes. Renewable and Sustainable Energy Reviews, 82, 1, February 2018, 837-844. URL https://www.sciencedirect.com/science/article/pii/S1364032117313448 (accessed 21/02/2018)

Miller, S.D., Heidinger, A.K., Sengupta, M., 2013. Chapter 3 – Physically Based Satellite Methods, in: Kleissl, J. (Ed),Solar Energy Forecasting and Resource Assessment. pp. 49–79. https://doi.org/10.1016/B978-0-12-397177-7.00003-6

Meteonorm, n.d. Irradiation Data for every place on Earth [WWW Document]. URL http://www.meteonorm.com/ (accessed 15/06/2017).

NOAA Office for Coastal Management, 2016. Spatial Trends in Coastal Socioeconomics (STICS): Total Economy of Coastal Areas. URL https://coast.noaa.gov/data/digitalcoast/pdf/qrt-coastal-economy-description.pdf (accessed 02/02/2018)

Padfield, T. 2013. NOAA Moisture Calculator. [WWW Document]. URL https://ready.arl.noaa.gov/READYmoistcal.php (accessed 23/06/2017).

Paulescu, M., Paulescu, E., Gravila, P., Badescu, V., 2013. Weather Modeling and Forecasting of PV Systems Operation. Green Energy Technol. 103. https://doi.org/10.1007/978-1-4471-4649-0

Perez, R., Cebecauer, T., Suri, M., 2013. Semi-Empirical Satellite Models, in: Kleissl, J. (Ed.), Solar Energy Forecasting and Resource Assessment. Academic Press, Boston, pp. 21–48. https://doi.org/10.1016/B978-0-12-397177-7.00002-4

Perez, R., Seals, R., Zelenka, A., 1997. Comparing satellite remote sensing and ground network measurements for the production of site/time specific irradiance data. Sol. Energy 60, 89–96. https://doi.org/10.1016/S0038-092X(96)00162-4

Polo, J., Wilbert, S., Ruiz-Arias, J.A., Meyer, R., Gueymard, C., Súri, M., Martín, L., Mieslinger, T., Blanc, P., Grant, I., Boland, J., Ineichen, P., Remund, J., Escobar, R., Troccoli, A., Sengupta, M., Nielsen, K.P., Renne, D., Geuder, N., Cebecauer, T., 2016. Preliminary survey on site-adaptation techniques for satellite-derived and reanalysis solar radiation datasets. Sol. Energy 132, 25–37. https://doi.org/10.1016/j.solener.2016.03.001

Pope, A., 2017. SRTM Slope DEM for Great Britain. https://doi.org/http://dx.doi.org/10.7488/ds/1720

Renard, F., 2017. Local influence of south-east France topography and land cover on the distribution and characteristics of intense rainfall cells. Theor. Appl. Climatol. 128, 393–405. https://doi.org/10.1007/s00704-015-1698-1

Ripley, B., 2002. rlm function | R Documentation [WWW Document]. URL https://www.rdocumentation.org/packages/MASS/versions/7.3-47/topics/rlm (accessed 10.16.17).

Ruiz-Arias, J.A., Quesada-Ruiz, S., Fernández, E.F., Gueymard, C.A., 2015. Optimal combination of gridded and ground-observed solar radiation data for regional solar resource assessment. Sol. Energy 112, 411–424. https://doi.org/10.1016/J.SOLENER.2014.12.011

Schroedter-Homscheidt, M., 2016. The Copernicus Atmosphere Monitoring Service (CAMS) Radiation Service in a nutshell. URL https://wdc.dlr.de/data_products/SERVICES/SOLARENERGY/Copernicus_radiation_service_in_nutshell_v5.pdf (accessed 02/02/2018)

Sengupta, M., Habte, A., Kurtz, S., Dobos, A., Wilbert, S., Lorenz, E., Stoffel, T., Renné, D., Gueymard, C., Myers, D., Wilcox, S., Blanc, P., Perez, R., 2015. Best Practices Handbook for the Collection and Use of Solar Resource Data for Solar Energy Applications 1–255. URL https://www.nrel.gov/docs/fy15osti/63112.pdf (accessed 02/02/2018)

Small, C., Nicholls, R.J., 2003. A Global Analysis of Human Settlement in Coastal Zones. J. Coast. Res. 19, 584–599. URL https://eprints.soton.ac.uk/39496/ (accessed 02/02/2018)

Strobel, M.B., Betts, T.R., Friesen, G., Beyer, H.G., Gottschalg, R., 2009. Uncertainty in Photovoltaic performance parameters - dependence on location and material. Sol. Energy Mater. Sol. Cells 93, 1124–1128. https://doi.org/10.1016/j.solmat.2009.02.003

Suri, M., Cebecauer, T., 2014. Satellite-Based Solar Resource Data: Model Validation Statistics Versus User'S Uncertainty, in: ASES SOLAR 2014 Conference. pp. 7–9. URL https://solargis.com/assets/publication/2014/Suri-Cebecauer--ASES-Solar2014--Satellite-Based-Solar-Resource-Data--Model-Validation-Statistics-Versus-User-Uncertainty.pdf (accessed 02/02/2018)

Šúri, M., Cebecauer, T., 2012. SolarGIS: Online Access to High-Resolution Global Database of Direct Normal Irradiance, in: Proceedings of the SolarPACES Conference. Marrakech, Morocco. URL https://solargis.com/support/publications/2012/presentation/solar-resource-assessment (accessed 02/02/2018)

UCAR, 2012. Cloud Types. URL https://scied.ucar.edu/webweather/clouds/cloud-types. (accessed 15/02/2018)

UK Met Office, 2006. MIDAS: UK Hourly Weather Observation Data. NCAS British Atmospheric Data Centre [WWW Document]. URL http://catalogue.ceda.ac.uk/uuid/916ac4bbc46f7685ae9a5e10451bae7c. (accessed 17/08/2016).

Wald,L., 2017. Synthesis Wald Nov. 2016, URL http://www.soda-pro.com/help/cams-radiation-service/validation/synthesis-wald-nov-2016 (access 06/02/2018)

Wetherald, R.T., Manabe, S., 1986. An investigation of cloud cover change in response to thermal forcing. Clim. Change 8, 5–23. URL https://link.springer.com/article/10.1007/BF00158967 (accessed 02/02/2018)

Yang, W.Y., Li, Z., Sun, T., Ni, G.H., 2016. Better knowledge with more gauges? Investigation of the spatiotemporal characteristics of precipitation variations over the Greater Beijing Region. Int. J. Climatol. 36, 3607–3619. https://doi.org/10.1002/joc.4579

Yordanov, G.H., Midtgård,O.M, Saetre, T.O., Nielsen, H.K.,Norum, L.E. 2013. Overirradiance (Cloud Enhancement) Events at High Latitudes. IEEE Journal of Photovoltaics, 3, 1, 271-277, DOI: 10.1109/JPHOTOV.2012.2213581

## Appendix A: Discussion of (Perez et al., 1997)

This work has been extensively referenced, having received over 176 citations to date (Google Scholar (Google, n.d.), January 2018). It received 61 citations in the 11-year period 2000-2010 as opposed to the average of 8 in the engineering field (Times Higher Education, n.d.). Post-2010, with widening availability of satellite data, the citation rate increased, reaching as high as 19 per year. Citing journals were published in English, French, Portuguese and Spanish. Most were in the field of photovoltaics, but there has also been interest from agricultural, terrestrial and oceanic sciences.

Approximately one-third of all citations study satellite modelling of irradiance. However, utilisation has broadened, particularly in the last three years. There has been a particular focus on photovoltaic electricity production. Other uses include merging ground-based and satellite irradiance data, irradiance forecasting, solar panel soiling and grid impacts of PV. Inputs into other disciplines include leaf area index and evaporation.

Half of all case studies citing (Perez et al., 1997) are based in Europe. Just two have a global application, Africa/Arabia and South America each comprise 15%, whilst Asia and North America contribute 5% respectively. Thus, although the original work was based on USA data, it has mostly been applied in Europe.

Despite the great number of citations, only two groups of researchers have attempted to emulate (Perez et al., 1997) work. (Martins and Pereira, 2011) obtained a break-even distance of 60 km for daily solar irradiance data in Brazil. Recent work on daily global horizontal irradiance (GHI) found the accuracy of the SARAH satellite model surpassed that of ordinary kriging interpolation of ground-based measurements when the distance to the closest measurement station exceeded 20 – 30 km (Urraca et al., 2016). This suggests that modern satellite models ought to deliver a much shorter break-even distance for hourly GHI than (Perez et al., 1997) figure of 34 km.

## Appendix B: Description of kriging technique used in this research

Kriging is widely used (Hofstra et al., 2008), suitable for data containing directional bias and provides error calculations. Specifically, ordinary kriging is used with an empirical semi-variogram. (The semi-variogram is a graph of the difference in value recorded at pairs of locations (the semi-variance) on the y-axis, plotted as a function of distance between them on the x-axis.) The semi-variogram model was selected as exponential, following an investigation of spatial autocorrelation, visual performance and cross-validation. Data from all the weather stations is utilised to calculate the end result. The empirical semi-variogram is fitted via the autofitVariogram technique from R software (Hiemstra, 2015). This obtains the sill and nugget from the semi-variance and the range from map size. (The sill is the value of semi-variance on the y-axis at which the exponential semi-variogram flattens. The nugget is the value at which the graph intersects its y-axis. Theoretically zero, the nugget value results from measurement errors, subsampling noise and fine-scale environmental variability. Additionally, it may include discontinuity of the data. In this instance, hourly solar radiation data may be discontinuous due to passing cloud. The range is the distance on the x-axis at which the model levels.) The R technique was chosen because of its ability to process the large quantity of data involved. The average nugget for all the hourly datasets is fairly large. This is caused by short-scale variability of irradiance in the UK. The country is located adjacent to the Afro-Eurasian land mass where several air masses converge. This causes the well-known changeability of the weather. (See (Palmer et al., 2017) for further explanation of selection of kriging and details of its application.)

The R Automap package provides automated kriging. Eighty semi-variograms (the number of weather stations) are computed for every hour for which data exists. That is 80 x number of daylight hours e.g. 5100 (12 x 365 plus extra dawn and dusk) = 408,000. Kriging took approximately 4 hours for one years' data using an i7 32 GB 8 core computer, using parallel computing and just-in-time compilation.

## Appendix C: Comparison of Atmospheric Input Data for Satellite Global Horizontal Irradiance Models

The differences in aerosol optical depth input data between the satellite models is charted in Figure C.1. The data was obtained by the authors from the CAMS and CM-SAF download sites. It can be seen in Figure C.1(a) that Solargis is very different to SARAH, CAMS less so. In Figure C.1(b) likewise, a substantial difference between CAMS and Solargis is visible. The differences are especially marked for sea salt, which is influential in the UK's maritime climate.  SARAH uses long-term monthly modelled averages for AODs, whereas Solargis employs daily calculated values. Long-term averages reduce variation in data, whilst higher temporal resolution calculated values fill gaps and reflect all changes, hence the disparity. CAMS takes satellite-derived 3-hourly AOD values which although shorter term, may still be subject to missing data.

(a)

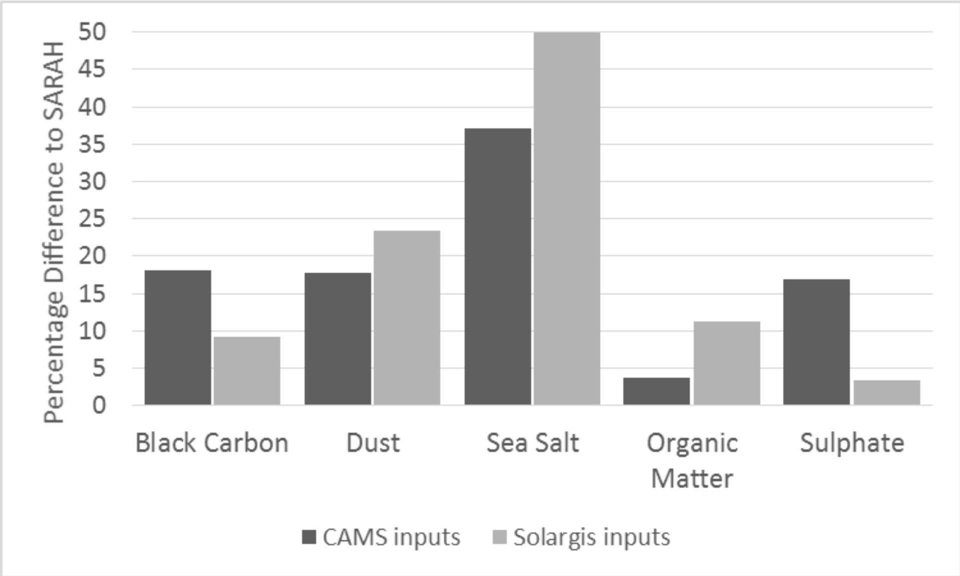


(b)

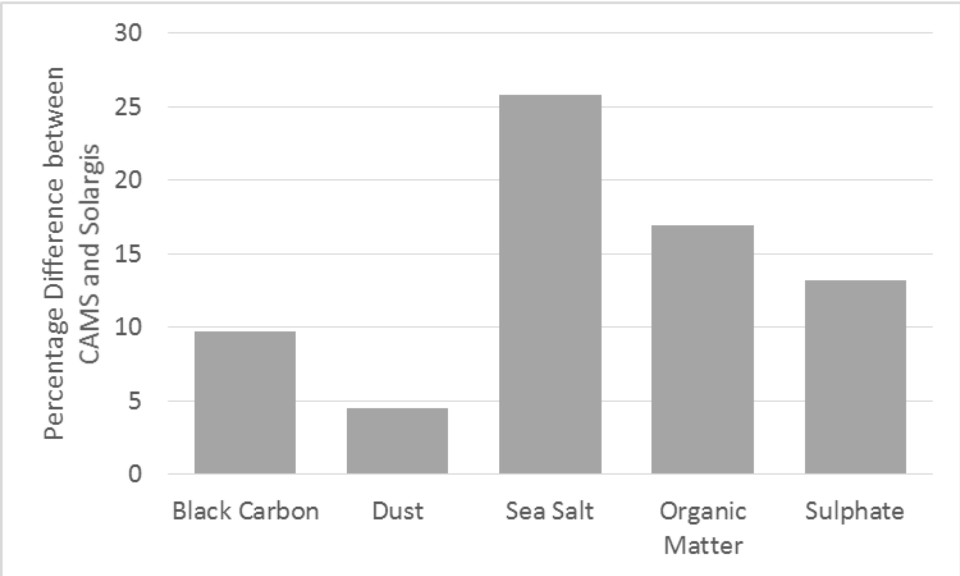


Figure C.1: Percentage Difference between satellite model partial aerosol optical depths at 550 nm. Location: East Midlands of UK. Time period: January 2010. (a) Difference between CAMS and Solargis partial AODs and those of SARAH. (b) Difference between CAMS and Solargis partial AODs